Transcriptional Regulation of Melanocortin 4 Receptor by Nescient Helix-Loop-Helix-2 and its Implications in Peripheral Energy Homeostasis

Umesh Deorao Wankhade

Dissertation submitted to the faculty of the Virginia Polytechnic Institute and State University in partial fulfillment of the requirements for the degree of

Doctor of Philosophy

in

Human Nutrition, Foods, and Exercise

Deborah J. Good, Chair

Dongmin Liu

Liwu Li

Robert W. Grange

Mathew Hulver

May 13th 2010

Blacksburg, VA

Keywords: Mc4r, Nhlh2, Transcription, white adipose, brown adipose, energy expenditure, obesity

Transcriptional Regulation of Melanocortin 4 Receptor by Nescient Helix-Loop-Helix-2 and its Implications in Peripheral Energy Homeostasis

Umesh Deorao Wankhade

ABSTRACT

Mutations in the melanocortin 4 receptor (MC4R) are the most frequent cause of monogenetic forms of human obesity. Despite its importance, the MC4R signaling pathways and transcriptional regulation that underly the melanocortin pathway are far from being fully understood. The transcription factor Nescient Helix Loop Helix 2 (Nhlh2), is known to influence the melanocortin pathway. It regulates the transcription of genes by binding to the E-Box binding sites present in the promoter region. Here in this dissertation, Nhlh2's role as a transcriptional regulator of Mc4r and the effects of deletion of Nhlh2 on peripheral energy expenditure, glucose homeostasis and fatty acid oxidation are reported. To investigate the transcriptional mechanisms of Mc4r and the involvement of Nhlh2, gene expression analysis, DNA-protein binding, transactivation assays, and SiRNA induction were used. We show that Nhlh2 regulates the transcription of Mc4r by binding to the three E-Boxes present on the promoter at -553, -361 and +47. Further, SiRNA knockdown of Nhlh2 in the N29/2 cell line depresses Mc4r expression which suggests the requirement of Nhlh2 for Mc4r transcription.

Development of adult onset obesity in the absence of evident hyperphagia questions the ability of mice which lacks Nhlh2 (N2KO) to utilize energy substrate efficiently. To test the effect of deletion of Nhlh2 in N2KO, body composition analysis, tissue specific characterization, fatty acid oxidation and glucose and

insulin homeostasis were assessed. N2KO mice have a higher fat content than WT at the age of 12 weeks. There are architectural differences in adipose tissue of N2KO. White adipose tissue (WAT) shows infiltration of macrophages, and increased mRNA and serum levels of interleukin 6 which suggests the presence of a systemic inflammatory state in the N2KO mice. Sympathetic nervous system tone is reduced in both brown adipose tissue (BAT) and WAT, as evidenced by gene expression analysis, and this may be because of overall reduced melanocortinergic tone in N2KO mice. N2KO mice have an impaired glucose tolerance on the basis of their late glucose clearance on glucose (non-significant) and insulin (significant) challenges. Fatty acid oxidation (FAO) is higher in red fibers of skeletal muscle, and the respiratory exchange ratio (RER) is lower in N2KO, which is indicative of using fat as a preferential energy source. Increased expression of genes involved in the lipid metabolism in skeletal muscle and liver supports the RER and FAO, and are indicative of high turnover of lipids in N2KO.

Findings from these studies implicate Nhlh2 as a transcriptional regulator of Mc4r which has a direct relevance to the ever increasing epidemic of obesity. Characterization of N2KO mice sheds light on the adult onset obesity phenotype. Knowledge gained from these findings will help us understand the monogenetic form of obesity more completely and could lead to the design of improved pharmacological therapies that target Nhlh2 or Mc4r or modify physical activity behavior.

This thesis is dedicated to

My Parents, Mrs Asha Wankhade and Mr Deorao Wankhade

for their continued support throughout my life

Acknowledgement

"Something that has always puzzled me all my life is why, when I am in special need of help, the good deed is usually done by somebody on whom I have no claim." This quote by William Feather reminds me of all the help and cooperation I received from my friends, mentor and committee members. I consider myself very fortunate to have people around me who have always helped me whenever I needed it without expecting anything in return. It is my pleasure to thank those people who made this thesis possible.

First of all I would like to express my sincere gratitude toward my advisor, Dr. Deborah Good. There was no way on Earth this thesis could have become a reality without her guidance and help. When Dr. Good gave me the opportunity to join her lab I was in a very difficult situation and I am indebted to her for my life for not only getting me out of that situation, but also making me a strong PhD candidate over the span of 3 years. Her continuous guidance and timely attention on my progress through weekly individual and lab meetings made me punctual with the research experiments and paper writings. Her encouragement for development in extracurricular activities such as serving as a student judge in various poster completions and inspiring me to participate in national and international level scientific conferences and meetings were very helpful to develop my personality overall. It was indeed a true pleasure working with her during these last three-and-a-half years.

I would like thank my committee for their timely guidance and valuable suggestions throughout the PhD. Dr. Hulver and Dr. Grange helped me

immensely with their expertise in muscle physiology. Dr. Hulver was especially helpful during indirect calorimetry and fatty acid oxidation experiments. Drs. Liu and Li always came up with valuable suggestions in the committee meetings which helped me perform my research in a better way. All of them were very flexible whenever I was deciding committee meeting timings. Without their guidance this thesis would not have been possible.

I would like to thank past and present Good lab members; without their co-operation and help it would have been very difficult to complete this thesis. Encouragement by Jacy, Numan, Risa, Haiyan and Karissa was a motivating force and light moments I shared with them in the lab were helpful in shading everyday stress. Especially Jacy was very, very helpful in correcting the manuscript I wrote for my papers and thesis. Former lab members, Dana Fox, Katherine Fawcett, Kristen Vella and Risa were very helpful when I started working in the lab initially. I would like to thank all of them for letting me incorporate their data for publication purposes. I could always call Dana if I had any question regarding the lab work and she was always helpful and prompt to answer. Risa help was very crucial when I was performing all the mouse work during my research.

Our lab set-up at the ILSB building requires us to work with other labs due to shared equipment. I would especially like to mention here that the Hulver lab, Hutson Lab and Schelmz lab were always considerate and I am very thankful to all of them for letting me use the core facilities whenever I needed them. Here

especially I would like to thank Ryan McMillan who did most of my fatty acid oxidation experiments.

I consider myself very lucky to have friends like Gaby, Pradyumna, Kapil, Pallavi, Roberto, Chandan, Sai, Amit, Sunil, Rajesh, Rajat, Jose, Heidi, Sebastian, Kavita, Aroon, Pratik, Laura, Vivek, Vishal and Jitendra. I cannot forget the contribution and help of Gaby and Roberto during progress towards my PhD. Talking to friends and sharing a cup of coffee indeed turned out to be a big stimulant to carry out my daily routine.

If I don't mention the name of Nicolin, my TA instructor, it would be an injustice. Whenever I was the TA for HNFE-3034, she was always helpful and considerate of any time constraints I had. Her flexibility regarding time schedules and her understanding nature has helped me immensely to give equal attention to both research and TA duties at the same time.

I would like to thank NIH for providing funding support to perform my research. I am also very thankful to the Department of HNFE for providing me funding support throughout the PhD.

My family's role in my accomplishments so far is hard to put into words. My parents, brothers Guddu, Sarika and Ravi were always there in hard times and good times. I cannot undermine the importance of their unbiased support during these last few years.

Finally I would like to express my sincere gratitude to THE ALMIGHTY GOD. I had no other place to go whenever I felt lost and wrong. Confessing in

front of you and praying everyday in front of you made my journey easy. Thank you for giving me the power to survive and excel through this path.

Thanks!!!

List of abbreviations

ACC-α	Acetyl-Coenzyme A carboxylase-α
ARC	arcuate nucleus
α-MSH	α-melanocyte stimulating hormone
ASM	Acid soluble metabolites
BAT	Brown adipose tissue
β-AR	B-Adrenergic receptor
CDC	Center for Disease Control and Prevention (CDC)
ChIP	Chromatin immunoprecipitation
CNS	central nervous system (CNS)
CPT-1α	Carnitine palmitoyl transferase
FAS	Fatty acid synthase
FFM	Fat free mass
GAPDH	Glyceraldehyde 3-phosphate dehydrogenase
GTT	Glucose tolerance test
HSL	Hormone sensitive lipase
LPL	Lipoprotein lipase
ITT	Insulin tolerence test
MC4R	Melanocortin 4 receptor (Human)
Mc4r	Melanocortin 4 receptor (mouse)
Mc4rKO	Mc4r Knockout Mc4rKO
NHLH2	Nescient helix-loop-helix 2 (Human)
Nhlh2	Nescient helix-loop-helix 2 (Mouse)
N2KO	Nhlh2 Knokcout mouse
Ndn	Necdin
PVN	paraventricular nucleus
PC1/3	Prohormone convertase 1/3
POMC	proopiomelanocortin
PPAR	Peroxisome Proliferator activated receptors
PGC	PPAR gamma coactivator
RER	Respiratory exchange ration
SNP	Single nucleotide polymorphisms
STAT-3	Signal transducer and activator of transcription 3
SCD	Steroyl Co A destaurase
SREBP1c	Sterol regulatory element binding protein 1
TRH	Thyroid releasing hormone
UCP	Uncoupling protein
WAT	White adipose tissue

Table of contents

Chapter 1

Introduction

During the past two decades there has been a tremendous increase in the obesity rate in United States, and worldwide. Despite ongoing efforts by both scientific organizations and public health officials, individuals fail to increase physical activity and reduce their energy intake to healthy levels suggested by government guidelines. According to Centers for Disease Control and Prevention (CDC), the Body Mass Index (BMI) range for a normal individual lies between 18.5 to 24.9 kg/m^2, whereas the range 25.0 to 29.9 kg/m^2 would classify an individual as overweight and a BMI equal to or greater than 30.0 kg/m^2 would classify an individual obese (1). The latest data released from CDC for the years 2007-2008 indicated that over 34% and 68% of total United States population are obese and overweight, respectively (2). The ever increasing epidemic of obesity is also responsible for significant financial costs. These costs include medical expenses to cover overweight , obesity and associated complications, and was 9.1% of total U.S. medical expenditures; the costs once reached as high as $78.5 billion in 1998 and $92.6 billion in 2002 (3). Along with the increasing percentage of obesity, related complications such as coronary heart disease, type 2 diabetes, cancers (endometrial, breast, and colon), hypertension (high blood pressure), dyslipidemia (for example, high total cholesterol or high levels of triglycerides) and stroke are also damaging human health at great extent.

Dramatic accretion in the worldwide obesity percentage can be attributed to different factors such as genetic make-up, environment, food habits, sedentary

lifestyles, and reduced levels of physical activity. Among the genetic factors responsible for causing obesity, single nucleotide polymorphisms (SNP) or other mutations in different genes controlling energy homeostasis and body weight maintenance directly or indirectly are responsible for the increasing cases of obesity due to genetic origin. Recently detected mutations in melanocortin 4 receptor (MC4R) have been associated with human obesity and reduced physical activity levels in up to 5.6% of the population (4, 5). The crucial role of MC4R in maintaining energy homeostasis and body weight regulation, accompanied by the high number of human carriers of MC4R mutations, makes MC4R one of the most important etiological factors of obesity of genetic origin.

The melanocortin pathway is an essential endocrine pathway, which is instrumental in maintaining body weight and energy expenditure. Mechanisms maintaining energy balance and body weight involve complex regulatory signal transduction pathways within the central nervous system, the gut and the fat depots of the body. Genes involved in energy homeostasis maintenance are regulated transcriptionally (i.e., promoter-mediated gene regulation) and post-transcriptionally (i.e., by post-transcriptional mRNA stability and protein translation). Despite being critical for energy homeostasis, the melanocortin pathway is not fully explored as far as its transcriptional regulation, downstream signaling and its tissue specific effects in overall body fat metabolism pathways are concerned. Therefore, it is necessary to explore the melanocortin pathway, its molecular physiology behind regulation of energy expenditure and body

weight maintenance to better understand the molecular and physiological basis of genetics origin of obesity.

In our laboratory, we study the transcription factor, Nescient helix-loop-helix 2 (Nhlh2), which belongs to the family of basic helix-loop-helix (bHLH) transcription factors. bHLH transcription factors bind to E-box sequences (CANNTG) and form heterodimers with other bHLH family members to enhance or depress the transcription of genes (6-8). The expression pattern of Nhlh2 varies depending on the energy status availability in the body (9). Nhlh2 co-localizes in 33% of the proopiomelanocortin (POMC) expressing neurons in the arcuate nucleus (ARC) and 41% of the TRH expressing neurons in the paraventricular nucleus (PVN) (9). In mice with the targeted deletion of Nhlh2 (N2KO mice), POMC mRNA expression is normal (10). However, POMC derived peptide, α-melanocyte stimulating hormone (α-MSH), is 50% reduced in protein levels in N2KO mice compared to WT mice (9, 10). Levels of Prohormone Convertase 1/3 (PC1/3) and PC2 are also reduced significantly, which is supported by the fact that PC1/3 is transcriptionally regulated by Nhlh2, in a co-regulatory complex with Signal transducer and activator of transcription 3 (STAT3). Reduced levels of α-MSH in N2KO mice are consistent with the fact that Nhlh2 regulates PC1/3 at transcriptional level, leading to reduced peptide processing of POMC. Reduced levels of melanocortin ligands such as α-MSH in N2KO mice, and transcriptional control over important genes such as PC1/3 by Nhlh2, suggest that Nhlh2 may have direct or indirect influence over the regulation of many genes and processes in the melanocortin pathway.

Earlier work from our laboratory has shown that targeted deletion of Nhlh2 in mice leads to adult onset obesity preceded by reduced physical activity levels (11, 12). Surprisingly, before the onset obesity, N2KO mice have normal food intake which suggests no problem with energy intake side of the equilibrium. However, increased body weight gain is indicative of impairment of in energy expenditure pattern. The established role of Nhlh2 in transcriptional regulation of PC1/3, reduced levels of endogenous melanocortin ligand such as α-MSH and development of adult onset obesity makes the N2KO mouse model perfect to study melanocortin pathway in detail. In the present two-phase study, we explored the role of Nhlh2 in transcriptional regulation of Mc4r and the downstream effects on energy expenditure and metabolism. In the first phase of the project, determination of Mc4r expression in N2KO mice and an examination of Nhlh2's transcriptional control of the Mc4r promoter were examined. In the second phase, the peripheral metabolic pattern in the N2KO mouse was examined using gene expression, a glucose-insulin homeostasis, and a fatty acid oxidation study. Findings from this research have direct relevance to understanding one of the major threats society currently faces: obesity and its complications. A detailed understanding of the genetic basis for obesity gained from the findings from this project will help to design best possible alternative therapeutic regimens or preventive strategies to treat this disorder.

Chapter 2

Specific Aims

Energy homeostasis, or the equilibrium between calorie intake and expenditure, is administered by neuroendocrine and autonomic pathways arising from, and controlled by, the central nervous system (CNS). Different neuronal populations in the ARC and the PVN play critical roles in maintaining the balance between energy intake and expenditure (13). The whole process of energy intake and expenditure is regulated transcriptionally (i.e., promoter-mediated gene regulation) and post-transcriptionally (i.e., by post-transcriptional mRNA stability and protein modification) as well as by subsequent signal transduction pathways activated and repressed by the protein products of the regulated genes. One of the transcription factors involved in the neuro-circuitry controlling body weight and energy expenditure is Nhlh2. Nhlh2 belongs to the family of bHLH transcription factors and is expressed in the ARC and PVN of the hypothalamus. Nhlh2, like other bHLH transcription factors, has a special binding affinity to E-Boxes (CANNTG) and forms heterodimers with other bHLH family members to regulate the transcription of genes (6-8). Nhlh2 is co-localized with leptin-receptors containing POMC and thyroid releasing hormone (TRH) neurons of the hypothalamus. Its expression is stimulated in response to leptin or food (10). In N2KO mice, PC1/3 levels are reduced by 50%, leading to a 40% reduction of α-MSH levels (10). Disrupted gene regulation at the CNS level can be transmitted to the peripheral tissues of the body through the sympathetic nervous system (SNS) (14) (Figure 1).

Nhlh2 as a transcriptional regulator of PC1/3 implicates its role in the processing of α-MSH, an endogenous ligand of the Mc4r. Promoter region of the Mc4r gene, which also possess E-Boxes, putative binding sites where Nhlh2 can bind and regulate the transcription. Functional polymorphisms in the Mc4r gene contribute to some of the most common causes of genetic obesity and to reduced physical activity in humans (5, 15, 16). Furthermore, two unrelated human families with obesity were recently shown to carry a polymorphism in the promoter of MC4R within an E-box motif that binds human NHLH2 (4). On the other hand, the N2KO mouse model shows adult onset obesity with reduced physical activity (11, 12). This phenotype is similar to the Mc4r knockout (Mc4rKO) mice or humans with functional polymorphism in MC4R (4, 17). Taken together, these data suggest a definite link between Mc4r expression and Nhlh2 and its role in the regulation of body weight.

The N2KO mouse model develops adult onset obesity mainly because of reduced physical activity which results in reduced energy expenditure (12). In the Mc4rKO mouse, defects in energy expenditure are evident in the form of differences in substrate utilization and nutrient partitioning (17, 18). The Melanocortin pathway controls glucose homeostasis and fatty acid metabolism (18, 19). Functional polymorphism(s)/mutation(s) may lead to disturbances in binding sites for Nhlh2, eventually disrupting normal melanocortin signaling in the N2KO mouse.

Our published data, as well as reports from other labs, clearly suggests that there is direct neuroendocrine control over peripheral cell metabolism and

which represents an important element of central nervous system control over adiposity (20, 21). Based on findings from the literature and from our lab, we propose that the disruption of the melanocortin signalling cascade in the central nervous system is due to the absence of Nhlh2, which leads to early adult onset obesity and disrupted glucose homeostasis and fatty acid metabolism in N2KO mice (10-12). We hypothesized that Nhlh2 regulates the melanocortin pathway at the transcriptional level by directly binding to the promoter of MC4R (Figure 1). As a consequence, N2KO mice have disrupted glucose homeostasis and fatty acid oxidation due to the lack of normal transcriptional regulation of Mc4r.

Specifically we propose:

1. To determine if Mc4r is a transcriptional target of Nhlh2

Polymorphisms/mutations in MC4R are one of the most common causes of genetic obesity and reduced physical activity in humans (5, 15, 16). Recently two unrelated human families with obesity were shown to carry a polymorphism in the promoter of Mc4r within an E-Box motif that binds human NHLH2 (4). These data clearly suggest a link between the requirement of Nhlh2 and Mc4r expression and its function. In this specific aim we asked the following key questions:

a) Are Mc4r mRNA levels altered in N2KO mice?

b) Does Nhlh2 bind to the putative binding sites in the Mc4r promoter region to regulate its transcription?

c) Does a mutation in one or more E-Box binding sites affect Mc4r transactivation in the presence of Nhlh2?

Transactivation assays, chromatin immunoprecipiation, electrophoretic mobility gel shift assays and qRT-PCR are the techniques were used to answer the above questions.

2. To determine the effect of Nhlh2 deletion on overall energy expenditure and glucose homeostasis: In the past we have shown that N2KO mice are physically less active which makes them obese at an early adult age. However, the absence of hyperphagia in these mice leads to questions about their ability to utilize energy substrates normally (12). Disrupted melanocortin signaling in Mc4r knockout mice alters glucose homeostasis and fatty acid metabolism (18, 22). Based on our previous observation that N2KO mice have reduced α–MSH and PC1/3 (23), we anticipated lower levels of Mc4r as well. We proposed here that the N2KO mouse has disrupted melanocortinergic tone, which mimics the effect of the targeted deletion of Mc4r. In this specific aim, we asked the following key questions:

a) Do N2KO mice have a normal glucose and insulin homeostasis?

b) Do N2KO mice have an altered energy expenditure pattern?

c) What are the downstream gene targets of the disrupted melanocortin pathway in N2KO mice?

We addressed the questions in this aim by studying the effects of Nhlh2 whole body deletion on energy expenditure patterns using whole body metabolic phenotyping, fatty acid oxidation, glucose and insulin tolerance tests, mRNA expression of genes involved in energy homeostasis.

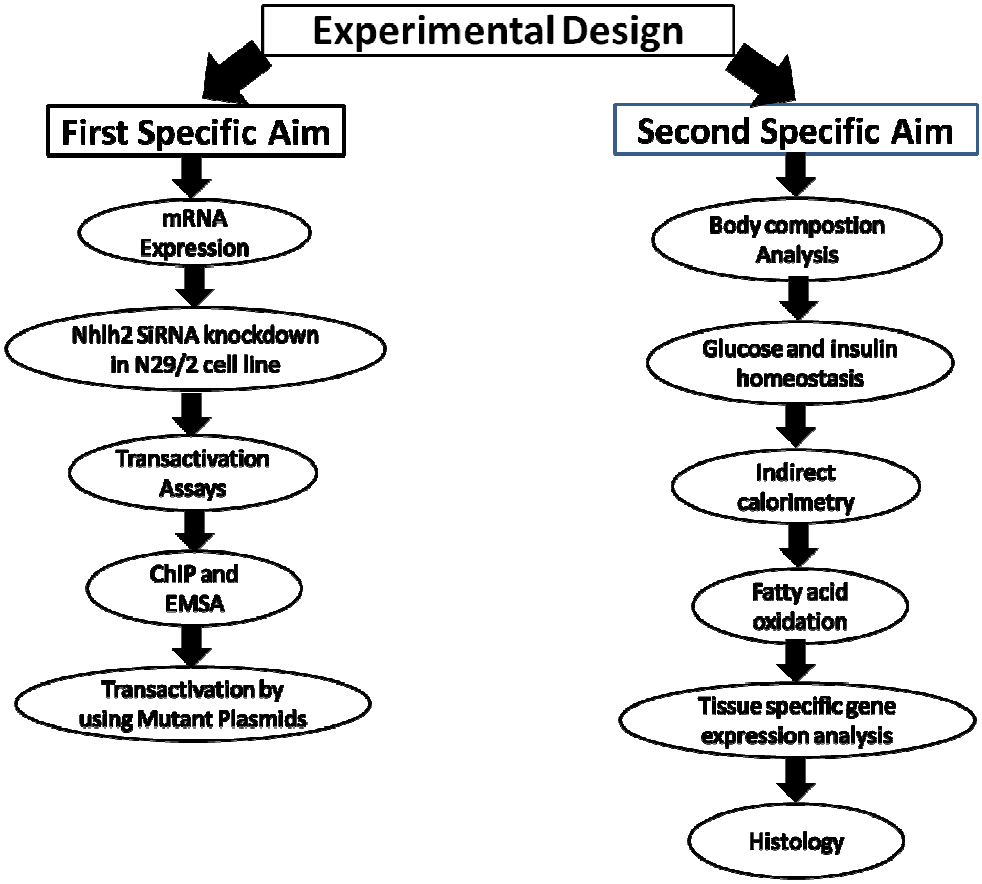
Experimental Design
First Specific Aim
mRNA Expression
Nhlh2 SiRNA knockdown in N29/2 cell line
Transactivation Assays
ChIP and EMSA
Transactivation by using Mutant Plasmids
Second Specific Aim
Body compostion Analysis
Glucose and insulin homeostasis
Indirect calorimetry
Fatty acid oxidation
Tissue specific gene expression analysis
Histology

Chapter 3

Melanocortin 4 Receptor is a Transcriptional Target of Nescient Helix-Loop-Helix-2

Umesh D. Wankhade, Katherine Fawcet and Deborah J. Good

Department of Human Nutrition, Foods and Exercise

Virginia Polytechnic Institute and State University, Blacksburg, VA 24061

Running title: Mc4r, a transcriptional target of Nhlh2

Key Words: NSCL-2, HEN2, Mc4r

Molecular Endocrinology (in preparation)

Introduction

Obesity-related traits such as body mass index (BMI), fat mass and leptin levels are 40-70% heritable (24-26). Mutations in genes controlling body weight and energy homeostasis are the largest contributing factor to genetic origins of obesity. The prevalence of obesity is 32.2% among adult men and 35.5% among adult women in the United States, which is significantly higher than what it was just a decade before (2). Changes in food habits and reduced physical activity are the two important environmental factors leading to today's increasing rate of obesity (27). However, it is crucial to consider the role of genetics in controlling body weight and energy homeostasis, especially with respect to the manner in which it contributes to the causes of obesity. Monogenic forms of obesity caused by polymorphism(s)/mutation(s) in genes such as carboxypeptidase E (CPE), Leptin, Leptin receptor, TUB, melanocortin 4 receptor (MC4R) and pro-opiomelanocortin (POMC) leads to impaired energy homeostasis (28-34). While single gene obesities obey the rules of Mendelian inheritance, these are rare when compared to the more common, polygenic form of obesity, in which many genes make minor contributions in determining the phenotype. Considering the importance of genetics in transmitting the traits to the next generation, detailed studies of the genetic aspects of this disorder are necessary to better understand the molecular physiology of obesity. Knockout mice provide a model for understanding the role that a single gene may play in the etiology of more complex human diseases.

Deletion of nescient helix-loop-helix 2 (Nhlh2) in mice results in adult-onset obesity with reduced exercise related energy expenditure (11, 12). Nhlh2 is a basic helix-loop-helix transcription factor which binds to the canonical E-box motifs for this family of transcription factors, CANNTG (7). Nhlh2 is predominantly expressed in the paraventricular (PVN) and arcuate nucleus of the hypothalamus (10), where its expression is modulated by energy availability (9, 35). One of the gene regulatory targets of Nhlh2 is the promoter for prohormone convertase 1/3 (PC1/3) (23). In response to leptin stimulation, Nhlh2 forms a heterodimer with the signal transducer and activator of transcription 3 (STAT3) transcription factor, leading to increased PC1/3 expression in hypothalamic neurons. As expected, N2KO mice have reduced expression of PC1/3 mRNA and neuropeptides of proopiomelanocortin (POMC) that would normally be processed by PC1/3, such as alpha melanocyte stimulating hormone (α–MSH) (10).

We have been actively trying to identify other possible targets of Nhlh2. In addition to mutations affecting the amino acid sequence of MC4R, several groups have identified mutations in non-coding regions of the gene. Of those, four are known to be in the 5' promoter region (36), with two of these polymorphisms potentially affecting the binding site for basic helix-loop helix transcription factors, including Nhlh2. The first of these two E-box mutations is found in both obese and non-obese controls at a frequency of 5%. This mutation -178 A/C, changes E-box #1 from CATCTG to AATCTG (36). The second mutation -20delGC ($MC4R^{\Delta GC}$) changes E-box #2 from CAGCTG to CA(del)TG

(4). This mutation was found in 2 extremely obese, but unrelated children and their relatives (4). The group who first identified mutation noticed that it was a perfect consensus site for NHLH2 and showed that indeed, human NHLH2 could bind to that E-box. However, they could not demonstrate transactivation differences between the normal and deleted promoter using a non-neuronal cell type (4). In fact, few studies have analyzed transcriptional activity of the normal human MC4R promoter. The only published study shows that the minimal promoter required for activity in neuronal and non-neuronal cells lines lies between -130 and +10, including E-box #2, the Nhlh2 binding site (37).

More than 70 different missense mutations have been identified to date and more than 90% of these mutations affect amino acids which are phylogenetically conserved (38). While it is clear that the melanocortin pathway and MC4R in particular, are instrumental in the regulation of body weight, MC4R transcriptional regulation is still largely unexplored. Determining the transcription factor(s) that regulate Mc4r must be conducted to better understand the control mechanisms for one of the most mutated genes leading to human obesity.

Results

Mc4r mRNA levels are reduced in N2KO mouse

mRNA expression levels of Mc4r were measured in N2KO and WT mice using quantitative RT-PCR (qRT-PCR) of RNA isolated from whole hypothalamus. Hypothalamic Mc4r mRNA levels were significantly reduced in N2KO mice compared to WT mice (Figure 1; *p≤0.05).

Knockdown of Nhlh2 in N29/2 cell line by siRNA reduces Mc4r expression

To determine the cell line to use to determine transcriptional role of Nhlh2, we tested Mc4r and Nhlh2 expression in N29/2 cell line. By using RT-PCR we determined that Nhlh2 and Mc4r are both expressed in N29/2 cell line (Figure 2A). SiRNA targeting of Nhlh2 mRNA was used to knockdown Nhlh2 expression in N29/2 cells. Cells containing the SiRNA targeted at Nhlh2 showed 83% reduced expression of the endogenous Nhlh2. This level of reduced Nhlh2 in N29/2 cells lead to a significant 97% reduction in endogenous Mc4r mRNA expression. GAPDH siRNA was used as a positive control and could knockdown GAPDH but had no effect on Nhlh2 or Mc4R levels. Likewise, scrambled siRNA did not affect expression of any of the tested genes (Figure 2B).

Putative binding sites for Nhlh2 are present on the Mc4r promoter

In humans, a MC4R promoter mutation which was detected at an E-box motif located at -450 has been associated with obesity in two unrelated families. This site can bind NHLH2 in vitro (4). The 4-fold reduction of Mc4r mRNA in N2KO mice suggests that Nhlh2 may have a positive role in regulating Mc4r

expression in mice. After analyzing the mouse Mc4r promoter, three different binding motifs for Nhlh2 represented by CANNTG were found at -553, -361 and +47 (Figure 3).

Nhlh2 positively regulates Mc4r promoter activity *in vitro*

The presence of Nhlh2 binding motifs in Mc4r promoter region combined with the reduced levels of Mc4r mRNA in N2KO mice, made it likely that Nhlh2 may directly transactivate the Mc4R promoter. The N29/2 cell line is an immortalized cell line used as a model of hypothalamic neurons (39). Mc4r and Nhlh2 are both expressed in N29/2 cells at basal levels. To test whether Nhlh2 transactivates the Mc4r promoter, an 803-bp fragment (–648 to +117) of the murine Mc4r promoter which has all three putative E-box motifs was subcloned into the pGL3 luciferase reporter plasmid (Fig. 2). Exogenous expression of Nhlh2 lead to significantly increased Mc4r promoter transactivation activity compared to basal levels (Figure.4). These results suggest that Nhlh2 is required for leptin-induced Mc4r promoter activity.

ChIP and EMSA reveals binding of Nhlh2 to all the three E-Boxes on the Mc4r promoter

Increased promoter activity of Mc4r in the presence of exogenously-expressed Nhlh2 confirmed the role of Nhlh2 in transcriptional regulation of Mc4r. However, positive induction of Mc4r promoter activity in the presence of Nhlh2 did not reveal the mechanism by which Nhlh2 regulates transcription of Mc4r. To determine whether Nhlh2 can bind to the Mc4r promoter and therefore directly affect Mc4r expression, a ChIP assay was performed on cells expressing myc-

tagged Nhlh2. Chromatin from N29/2 cells was immunoprecipitated using an anti-myc antibody to pull down all regions bound to the N2-myc fusion protein. Primers to the Mc4r promoter region which amplify a region of DNA containing all the three putative E-box motifs were then used to detect the immunoprecipitated chromatin. As shown in Figure 5A, this Mc4r promoter region containing the putative E-box motifs was pulled down by the antibody to c-myc, indicating that N2-myc was occupying the endogenous chromatin region where the Mc4r promoter is located. PCR was also performed on a Mc4r promoter plasmid and the ChIP input material as positive controls (Figure 5A). Cells not transfected with Nhlh2-myc as well as a no-antibody control were included as negative controls (Fig. 5A).

ChIP assays confirmed the binding of Nhlh2 to the Mc4r promoter. However, it did not reveal the actual binding site for Nhlh2. To specifically identify which of the three E-box motifs that Nhlh2 was interacting with, electrophoretic gel mobility shift assays (EMSA) were performed. Three different oligo-nucleotides (TABLE 1) for each of the three E-Box sites in Mc4r promoter were used for EMSA. Oligonucleotides designed to the E-Box motif present on the necdin promoter were used as a positive control. Binding of Nhlh2 and necdin promoter has been documented (40). Nuclear extract prepared from N29/2 cells transfected with Nhlh2-myc showed that necdin and all the three E-Boxes bind Nhlh2 (Figure 5B Lane e). Oligonucleotides with a mutation did not bind, or showed reduced binding to Nhlh2 (Figure 5B Lane f). Nuclear extract not transfected with Nhlh2-myc showed no binding to Necdin and 1st ('CAAATG' -

553) and 2nd E-Box ('CAGCTG' -361) with wild type or mutant Oligonucleotides (Figure 5B, Lanes g - h). However, the third E-Box (+47) showed binding in nuclear extract not transfected with Nhlh2 (Figure 5B, Lane g). Binding of the third E-Box may indicate involvement of a transcription factor other than Nhlh2. As the N29/2 cell line itself expresses many of the transcription factors endogenously (Wankhade and Good unpublished). Competition analysis with excess cold Oligonucleotides confirmed that this binding (Figure 5B, Lane e) was specific (Figure 5B, Lane i).

Nhlh2 requires all three E-Box motifs to induce promoter transactivation of Mc4r in N29/2 cell line

ChIP and EMSA showed that Nhlh2 binds to all three E-Boxes located in Mc4r promoter. Mutation was created by using site directed mutagenesis to determine the effect of mutation in individual E-Boxes on overall transactivation of Mc4r in presence of Nhlh2 (Figure 6A). Mutation of first E-Box (Mc4r-Mut-1), second E-Box (Mc4r-Mut-2) and third E-box (Mc4r-Mut-3) led to significant reduction of promoter activity as compared to WT (Figure 6B). Mc4r-Mut-1 promoter showed almost no transactivation compared to WT Mc4r promoter (**$p \leq 0.01$). Mc4r-Mut-2 and 3 showed better transactivation rate than increased promoter activity than Mc4r-Mut-1, but still was significantly reduced as compared to WT Mc4r promoter (**$p \leq 0.01$). Although mutation in individual E-Boxes led to various degree of reduction of promoter activity, synergistic action of all three E-Boxes is needed for full promoter induction in presence of Nhlh2.

Discussion

The role of melanocortin pathways in body weight maintenance and energy homeostasis is well documented. The results presented here identify a new regulatory target for the basic helix-loop-helix transcription factor Nhlh2, placing it as a critical upstream regulator of melanocortin signaling through direct transcriptional regulation of the Mc4r gene.

Several other genes are known targets of Nhlh2. For example, Nhlh2 binds to an E-box motif (TT**CATGTG**GG) on the proximal promoter of necdin (NDN) (40). Ndn regulation by Nhlh2 positively regulates development of gonadotropin hormone releasing hormone neurons in the hypothalamus (40). N2KO mice are hypogonadal with reduced sexual activity (11, 41) providing a strong link between Nhlh2 transcriptional regulation of Ndn and sexual development.

Nhlh2, forms a heterodimeric complex with STAT3, to coordinate the regulation of the PC1/3 gene at an overlapping STAT:E-box motif on the PC1/3 promoter (TTATATT**CAAATG**) (23). Reduced expression of PC1/3 in N2KO mice leads to reduced synthesis of one of the fully processed POMC peptides, α-MSH, and the thyrotropin-releasing hormone (TRH) peptide. Our new results suggest that deletion of Nhlh2 has a double effect on melanocortin signaling, reducing both levels of the receptor and the peptide which binds the receptor.

These results identify a new transcriptional target for Nhlh2. In addition results also indicate both new and confirmed E-box motifs that interact with Nhlh2. E-box#1 at -553 (CAAATG) on the mouse Mc4r promoter is identical to the E-box identified for the PC1/3 promoter (23). E-box #2 (CAGCTG) has

previously been found to bind Nhlh2 in a complex with Bex2 and LMO2, although a specific gene that is regulated by this complex was not identified by the study which used all synthetic promoters (42). The sequence of E-box #2 at -361 is identical to that E-box in the human MC4R promoter which when mutated by a 2-bp deletion is linked to obesity in two different human cohorts (4). E-box #3 (CAGATG) at +47 in the Mc4r promoter region, is a novel Nhlh2 binding motif, and is interesting in that it is found past the transcriptional start site of Mc4r.

A promoter reporter construct, which has individual E-Box mutations at all three sites led to none or significantly reduced promoter induction. The first E-Box (CAAATG) mutation led to no promoter activation in the presence of Nhlh2. These results are actually consistent with the earlier reports where the CAAATG E-Box sequence was shown to have one of the highest affinities for Nhlh2, among other E-Boxes (42). The second E-Box (CAGCTG) and third E-Box (CAGATG) mutations also led to significantly reduced promoter transactivation. These results suggest that all three E-Boxes are critical for Mc4r transcription.

Reduced expression of melanocortin signaling in N2KO mice is hypothesized to lead to reduced sympathetic nervous system (SNS) outflow to peripheral tissues including adipose (Wankhade et al., submitted) and increased body weights in mutant animals. Mutations in either PC1/3 or MC4R in humans lead to obesity, implicating NHLH2 as a key controller of genes relevant to human body weight control.

Material and methods

Experimental animals

All animal protocols were approved by the Institutional Animal Care and Use Committees at the Virginia Polytechnic Institute and State University. Animal colony maintenance, breeding and genotyping have been described previously (10). N2KO and normal mice were maintained in 12 h light, 12 h dark conditions with *ad libitum* access to food (4.5% crude fat) and water. Only male mice were used for all experiments, to eliminate the need for estrous cycle analysis in female mice (WT N=12, N2KO N=10). All mice were euthanized by CO_2 asphyxiation at 13.00 h to standardize hormone and steroid levels that fluctuate hourly.

Quantitative real-time PCR (QPCR) from whole hypothalamus

After euthanization, brains were isolated by dissection. A hypothalamic block, Mouse Brain Matrix (Zivic Laboratories Inc., Pittsburgh, PA, USA) was used to properly dissect the hypothalamus. The brain segment was put into 4 M guanidine isothiocyanate buffer and homogenized. Samples were layered over 5.7 M cesium chloride buffer and spun for 18 h at 120,000 g at 20 ℃. The supernatant was discarded and RNA was resuspended in DEPC water. RNA was then DNAse treated. cDNA was created using reverse transcriptase in a magnesium buffer (Promega Corporation, Madison, WI, USA) for 1 h at 42 ℃. Quantitative real-time PCR (QPCR) for Mc4r expression in the hypothalamus was performed using Mouse Mc4r primers (TABLE 1). Mouse β-actin was used as a housekeeping control gene. QPCR was performed by using the 7900HT

PCR system and the Power SYBR Green PCR Master Mix (Applied Biosystems, Foster City, CA, USA). mRNA levels of Mc4r were normalized against β-actin. Normalized levels of mRNA were measured in triplicate per individual mouse from which sample means were calculated for each mouse. Data are reported as the fold-difference from the WT *ad lib* fed experimental group. For each mRNA amplified, melting curve analysis was done to confirm the presence of a single amplicon. The data presented are means ± SE *p< 0.05, **p<0.01.

Inhibition of Nhlh2 using Small Inhibitory RNA

The N29/2 cell line possesses endogenous Nhlh2 expression. To knock down Nhlh2 expression, we used SiRNA transfection by targeting the coding region of Nhlh2. Silencing of Nhlh2 expression was accomplished using *Silencer*® select predesigned siRNA (Ambion Austin TX) targeted to the coding region (sense-5'AGAUCGAGAUUCUGCGCUUtt-3', antisense-5'AAGCGCAGAAUCUCGAUCUtg-3'). *Silencer*® Select GAPDH siRNA (catalog# 4390849) (Ambion, Austin, TX) was used as a positive control. *Silencer*® Select Negative Control siRNA (catalog# 4390843) (Ambion, Austin, TX) was used as a negative control. Cells were transfected using HiPerfect (Qiagen, Valencia, CA), SiRNA transfection reagent and after 24 hrs were collected for RNA isolation with Trizol method.

cDNA was created using reverse transcriptase in a magnesium buffer (Promega Corporation, Madison, WI, USA) for 1 h at 42 ℃. Quantitative real-time PCR (QPCR) for β–actin, GAPDH, Mc4r and Nhlh2 expression was

performed using their respective primers (TABLE 1). QPCR was performed by using the 7900HT PCR system and the Power SYBR Green PCR Master Mix (Applied Biosystems, Foster City, CA, USA). mRNA levels of Mc4r were normalized against β-actin. Normalized levels of mRNA were measured in triplicate per individual well per treatment from which sample means were calculated for each mouse. Data is reported as the fold-difference over negative control. For each mRNA amplified, melting curve analysis was done to confirm the presence of a single amplicon. The data presented are means ± SE *p< 0.05, **p<0.01.

Plasmid reporter construct

The plasmid reporter construct containing the Mc4r promoter was a gift of Kathleen Mountjoy, University of Auckland, New Zealand. It was prepared from 1098 bp of mouse MC4R promoter sequence and 426 bp of 5′ untranslated region (UTR) inserted into pGL3 basic (Promega, Madison, WI) (37). By using the above plasmid we prepared a shorter reporter construct by amplifying an 800 bp region which contained all three E-Box sites of the Mc4r promoter. Primers used are listed in Table 1. The HindIII sites in the forward and reverse primer were used to insert the PCR-generated 800bp Mc4r fragment into the pGL3 basic vector by using a site between the luciferase coding sequence and the SV40 polyadenylation sequence. The resulting plasmid was prepared using a Qiagen Maxi Plasmid kit (Qiagen Ltd., Valencia, CA). The plasmid constructs containing STAT-3, and leptin receptor (ObRB) were a generous gift from,

respectively, Dr. James Darnell, The Rockefeller University, New York, NY, and Christian Bjørbæk**,** Harvard Medical School, Boston, MA.

Site directed mutagenesis

The Mc4r E-Box mutant constructs were generated by using PCR-Site directed mutagenesis. PCR reaction was performed by using Platinum *Pfx* DNA Polymerase (Invitrogen) along with WT Mc4r promoter construct as a template with a 5 min. elongation time. Primer sequences (Table 1) with mutations designed for each individual E-Box site were used. The PCR cycle used was; denaturation step- 15 seconds at 94^0 C, annealing- 55^0 C for 30 and elongation time 1kb/min. PCR amplification was confirmed by running 5 ul of PCR product stained with Ethidium Bromide (EtBr) run on a 1% agarose gel and visualized under UV light. Subsequently, the PCR product was digested with *DpnI* to remove any template DNA. After visualizing DNA on the 1% agarose gel with the help of EtBr, the *DpnI*-digested PCR product was transformed, miniprepped and sequenced at the Virginia Bioinformatics Institute.

Cell culture and transfections

The hypothalamic N29/2 cell line (Cellutions Biosystems, Toronto, Ontario) were maintained in Dulbecco's modified Eagle's medium (DMEM) supplemented with 10% fetal bovine Serum 100 units/ml penicillin, and 10ug/ml streptomycin (HyClone, Logan, UT) at 37℃ in 5% CO_2. Cells were transfected using Effectene transfection reagent (Qiagen, Valencia, CA) according to the recommendations by the manufacturer. Briefly, cells were plated into 12-well plates at a concentration of $2X10^5$ cells/ml 24 hours before transfection and were

transfected with 535ng of DNA per well (200ng reporter Mc4r plasmid; 35ng of CMV-β-gal plasmid; and 100 ng each of the Nhlh2, Stat3, ObRb and/or empty vector (pcDNA-zeo). The CMV-β-gal plasmid was used as the internal control to check the transfection efficiency. Transfections were reproduced in triplicate. In all transfections, total input DNA was kept constant and controlled by using the empty vector where appropriate.

Luciferase and β-galactosidase Assays

24 hours after transfection, N29/2 cells were serum starved overnight. Cells were then treated with either 1.2 ug of leptin or vehicle (PBS)/ml of serum-free media for 2 hours. Two hours after stimulation, cells were lysed in 300μl Reporter Lysis Buffer (Promega) according to the manufacturer's recommendations. A 5 μl aliquot was used for the luciferase (luciferase assay system, Promega, Madison, WI) and a 20ul aliquot was used for β-galactosidase assays (Promega, Madison, WI). For each assay, the basal WT promoter total luciferase activity normalized against β-galactosidase activity was taken to be 1, and results were expressed as fold activation over the control value. The data presented are means ± SE (*$p < 0.05$) of three of more independent experiments.

Chromatin Immunoprecipitation Assay (ChIP)

ChIP assays were performed using the Chromatin Immunoprecipitation (ChIP) kit (Upstate, Charlottesville, VA) according to the manufacturer's recommendations. Cells were transfected with Nhlh2-myc (a gift from Dr. Thomas Braun, University of Halle-Wittenberg, Germany) and STAT3 and

treated with leptin for 15 minutes. Proteins bound to DNA were cross-linked using formaldehyde at a final concentration of 1% for 15 minutes at 37℃. Protein-DNA complexes were immuno-precipitated using 1mg myc-tag mouse monoclonal primary antibody (Cell Signaling, Danvers, MA). Nhlh2-myc promoter complexes were measured by PCR. The primers (TABLE 1) flanking the region of the Mc4r promoter where all three E-Boxes are located were used for PCR amplification. The samples were electrophoresed using a 1% agarose gel, and visualized by ethidium bromide staining.

Electromobility Shift Assay (EMSA)

Oligonucleotides were annealed and labeled with T4 polynucleotide kinase (Promega, Madison, WI) and [γ-^{32}p] deoxy (d)-ATP (PerkinElmer, Waltham, MA; 3000 Ci/mmol). Oligonucleotides used for EMSA analysis are listed in TABLE 1. Labeled oligonucleotides were used as probes or remained unlabeled as competitors. A total of 5μg protein was incubated with 35fmol of [γ–^{32}p] dATP-labeled probe in binding buffer (Promega) for 10 minutes at room temperature. For competition experiments, a 10-fold molar excess of unlabeled oligonucleotide was added to the binding reaction. DNA-protein complexes were separated from free DNA by electrophoresis on a 6% non-denaturing polyacrylamide gel. All gels were pre-run in 0.5X Tris-borate-EDTA buffer for 30 minutes prior to electrophoresis at 25V for 1-2 hours. Gels were dried under vacuum and exposed to film (Eastman Kodak, Rochester, NY).

Figure legends

Figure 1: Hypothalamic Mc4r mRNA levels in WT and N2KO mice

Whole hypothalamic RNA was isolated from WT and N2KO animals that were given *ad libitum* access to food and water. Relative expression levels of Mc4r RNA, which were measured using qRT-PCR and normalized to β-actin, are shown. The results are expressed as mean ± SE; *p< 0.05; (WT N= 12 and N2KO N=10 animals).

Figure 2: SiRNA knockdown of Nhlh2 in N29/2 cells reduces Mc4r expression

A. The N29/2 cell line expresses Nhlh2 and Mc4r endogenously. By using RT-PCR, Nhlh2 and Mc4r expression is determined. Control refers to the PCR with tail DNA samples.

B. SiRNA was used to knockdown the endogenous Nhlh2 expression in the N29/2 cell line. As a positive control, GAPDH SiRNA was used. Scrambled siRNA was used as a negative control. After transfection cells were collected and used to isolate mRNA. qRT-PCR was used to determine the mRNA expression. β-actin was used as normalizing control. The results are expressed as mean ± SE; *p< 0.05;

Figure 3: The Mc4r proximal promoter region

An 803-bp fragment (–648 to +117) of the murine Mc4r promoter was cloned into the pGL3 basic plasmid and used for luciferase reporter assays. The

three putative Nhlh2 binding sites (*squared in gray*) are numbered serially towards the transcription start site.

Figure 4: Mc4r promoter activity is enhanced in presence of Nhlh2 in transactivation assays

Activity of the WT Mcr4-luc reporter transfected into N29/2 cells in the absence (*gray bars*) or presence (*black bars*) of Nhlh2. Luciferase activity was measured and normalized to the expression of β-gal-encoding protein. Normalized activity is presented relative to the values obtained in cells transfected with empty vector PGL-3-luc alone ± SE; **$p < 0.01$.

Figure 5: ChIP and EMSA reveal Nhlh2 binds all three E-Box motifs on the Mc4r promoter

A. ChIP assay demonstrating binding of Nhlh2-myc to the Mc4r promoter. Lane a, PCR positive control using Mc4r plasmid; Lane b, the input included in the PCR represents 10% of the total chromatin. Lane c, A ChIP of cells not transfected with Nhlh2-myc was included as a negative control. Lane d. the Mc4r promoter immunoprecipitated with the Nhlh2-myc chromatin complex.

B. EMSA experiments demonstrating binding of Nhlh2 to all three E-box binding sites and positive control Necdin. The positive control Necdin, E-box motif at –553 (CAAATG), E-box motif at –361 (CAGCTG) and E-box motif at +47 (CAGATG) on Mc4r promoter binds to Nhlh2 (Lane a). Mutant Oligonucleotides for each of the sites mentioned above fails to bind or shows reduced binding (Lane b). WT and Mutant Oligonucleotide by using nuclear extract not

transfected with Nhlh2 E-Boxes except the E-Box located at +47 (Lane b and c). 10X competition (Lane e)

Figure 6: All three E-Box motifs on Mc4r promoter are critical for its full transactivation in presence of Nhlh2

A. Substitution mutations in all three E-Box sites were made. Mc4r-WT plasmid has a promoter region with all the three E-Boxes intact. Plasmids containing the promoter with mutations at -553, -361, and +47 are stated as a Mc4r-Mut-1, Mc4r-Mut- 2 and Mc4r-Mut-3, respectively.

B. Transactivation assays performed by using WT Mc4r promoter and with the promoter with mutations in each individual E-Box motifs. Activity of the WT Mc4r-luc reporter (WT) transfected into N29/2 cells in the presence (*black bars*) or absence (*gray bars*) of Nhlh2. Cells were transfected with the indicated Mc4r-luc reporter, Nhlh2, and mutated plasmids as stated. The luciferase activity was measured and normalized to the expression of β-gal-encoding protein. Activity is presented relative to the values obtained in cells transfected with PGL3-luc alone ± SE. **, $p < 0.01$; to empty vector expression.

Table 1: Primer sequences

All the sequences used and their purpose are listed below with the sequence ordered 5'-3'.

Primer	Sequence 5'--3'	Purpose
Mc4r forward	GGAAGATGAACTCCACCCACC	qRT-PCR & ChIP
Mc4r reverse	AATGGGTCGGAAACCATCGTC	
β-actin forward	GGAATCCTGTGGCATCCAT	qRT-PCR
β-actin reverse	GGAGGAGCAATGATCTTGATCT	
Mc4r Promoter Forward	GGCCAAGCTTGTTCACAGGCAATACGCTTTC	Plasmid reporter construct
Mc4r Promoter Reverse	GGCCAAGCTTTTCTCTCTCTCTCAGTGCGGC	
Mc4r E-Box Site 1 Sense	GCAGAAACTGCAAATGGAGAAACAGCT	EMSA
Mc4r E-Box Site 1 antisense	AGCTGTTTCTCCATTTGCAGTTTCTGC	
Mc4r mutant E-Box Site 1 Sense	GCAGAAACTGCATGGAGAAACAGCT	
Mc4r mutant E-Box Site 1 antisense	AGCTGTTTCTCCATGCAGTTTCTGC	
Mc4r E-Box Site 2 Sense	GGAGCCAGGACAGCTGCTTTTCATTTC	
Mc4r E-Box Site 2 antisense	GAAATGAAAAGCAGCTGTCCTGGCTCC	
Mc4r Mutant E-Box Site 2 Sense	GGAGCCAGGACATGCTTTTCATTTC	
Mc4r Mutant E-Box Site 2 antisense	GAAATGAAAAGCATGTCCTGGCTCC	
Mc4r E-Box Site 3 Sense	TGTGGGCGCGCAGATGCAGACGCGGCT	
Mc4r E-Box Site 3 antisense	AGCCGCGTCTGCATCTGCGCGCCCACA	
Mc4r Mutant E-Box Site 3 Sense	TGTGGGCGCGCATGCAGACGCGGCT	
Mc4r Mutant E-Box Site 3 antisense	AGCCGCGTCTGCATGCGCGCCCACA	
Necdin sense	GGGCCCTCATTTTCATGTGGGGCC	
Necdin antisense	CCCCCAGGCCCCACATGAAAATGA	
Necdin mutant sense	GGATGGGTGCGTGGGGCC	
Necdin mutant antisense	GGCCCCACGCACCCATCC	
E-box site 1 mutant sense	CCGTTAGAGCAGAAACTGCAACGGGAGAAACAGCTACCAGCACG	Site Directed Mutagenesis
E-box site 1 mutant anti-sense	CGTGCTGGTAGCTGTTTCTCCCGTTGCAGTTTCTGCTCTAACGG	
E-box site 2 mutant sense	GCCTGCTTCGGGAGCCAGGACAGAGGCTTTTCATTTCTTTTTTTTAT	
E-box site 2 mutant anti-sense	ATAAAAAAAAGAAATGAAAAGCctCTGTCCTGGCTCCCGAAGCAGGC	
E-box site 3 mutant sense	GCGGTGTGAGTGTGGGCGCGCAGCGGCAGACGCGGCTCCCAGCA	

E-box site 3 mutant anti-sense	TGCTGGGAGCCGCGTCTGCCgCTGCGCGC CCACACTCACACCGC	
Nhlh2 Forward	CAGTTGGCGTGAAGAGGTAGA	qRT-PCR
Nhlh2 Reverse	AATGCCCACGAGAAATACCA	
GAPDH Forward	AGGTCGGTGTGAACGGATTTG	
GAPDH Reverse	TGTAGACCATGTAGTTGAGGTCA	

Figure 1

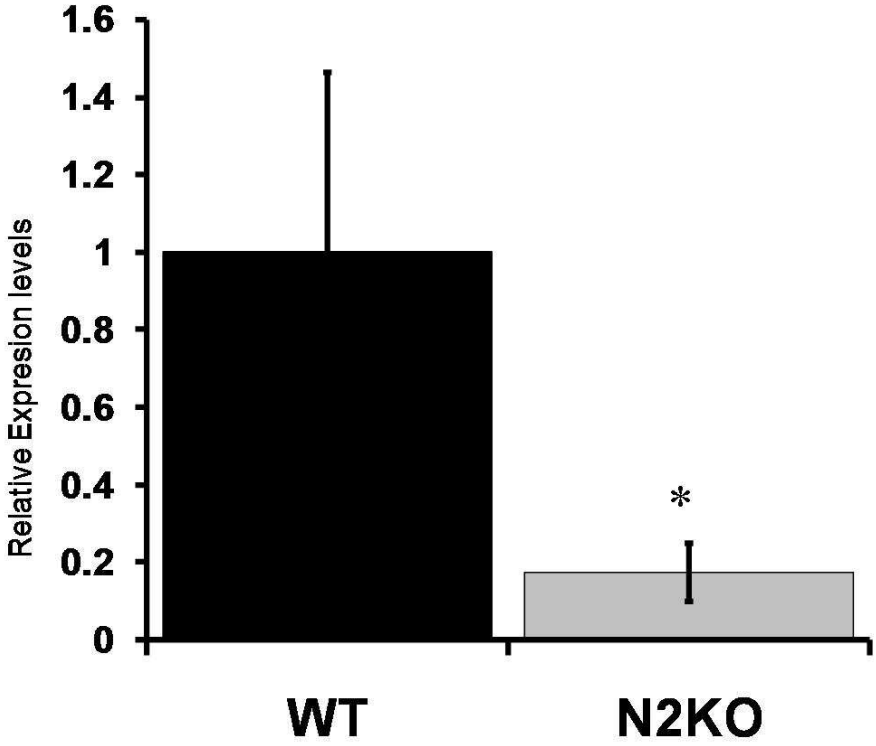

Figure 2

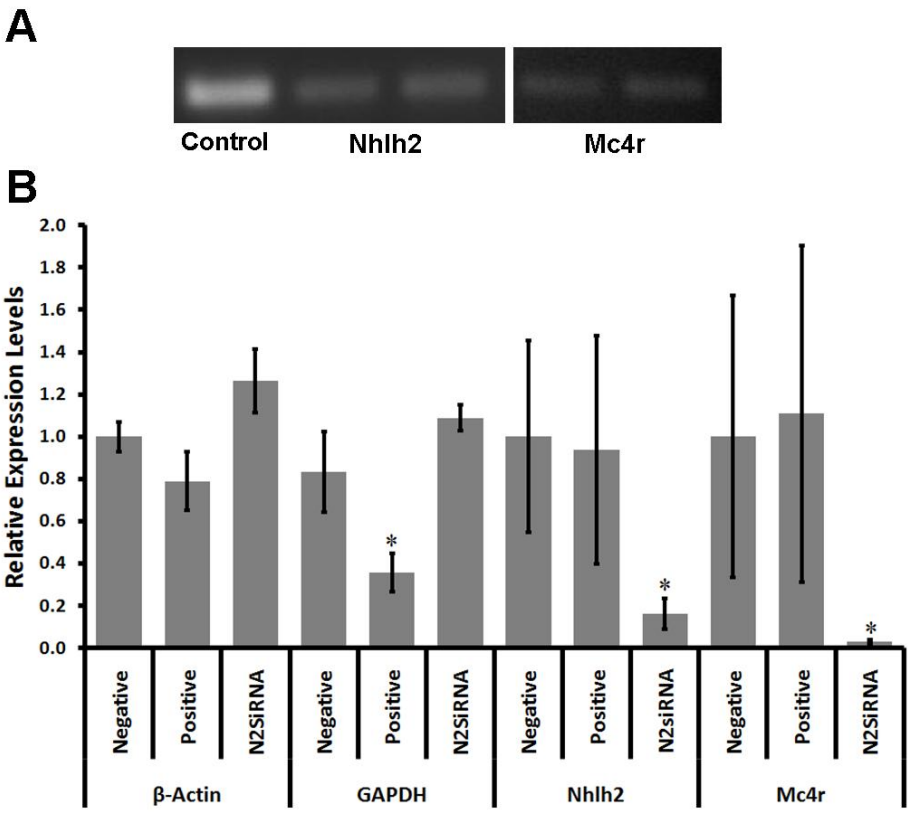
A
Control
Nhlh2
Mc4r
B
Relative Expression Levels
2.0
1.8
1.6
1.4
1.2
1.0
0.8
0.6
0.4
0.2
0.0
Negative
Positive
N2SiRNA
β-Actin
GAPDH
Nhlh2
Mc4r
N2siRNA
*

Figure 3


-648 GTTCACAGGCAATACGCTTTCACAAATGCCACTTGAACTTTTAAAAATACA
-597 GGGAATGACCACTTTTCCAGCCGTTAGAGCAGAAACTGCAAATGGAGAAAC
-546 AGCTACCAGCACGCAAGAAGTGAACCTGGTCTTAATCTCTGGCTTTGCTGT
-495 AATTCTCCACAGCATACTCATCTATTTAATTAAATTACTGCCTGCATTTCT
-444 AGTCTTTCAAACTGAGCCTTCCGTCATTCAGGGGGGCATCCTGGGCAGAGG
-393 GGCAGCGCCTGCTTCGGGAGCCAGGACAGCTGCTTTTCATTTCTTTTTTTT
-342 ATCCACAATCACGCATGAGTTCAGTCTCAAGGAGGAAAGAGCCTGGCTGAT
-291 TCCCGAGGATTTCAGGAGTATCTCAGAATGTGCTCGAGCAATCAAGTCATT
-240 TCTCTTATAACTTGGAAAGGAAAATCCCGTGATACCTTCCCACCCCAGCAG
-189 CCCTAGCCACTGAGCCGGTTGCTGCGCTGTAATCTATCTGTGCAAGATCGA
-138 TGTCTCAGAACCACTGAATACGGATTGGTCAGAAGGAAGCAGAGGAGGAGC
-87 CATTCAGAACACCCCCCACCCCCCGGCCCCCCTCCGTCTAACCATAAGAAA
-36 TCAGCAGCCCGCACTAGGCTGCTCTGGCTCACAAAGATGCTCAGGAAGCTG
+15 AACTTCTGAGAGGCTGCGGTGTGAGTGTGGGCGCGCAGATCCAGACGCGGC
+66 TCCCAGCAGTACAGCGAGTCTCAGGGAAAAGGACTCTGAAAAGACCCCGAG
+117 TGAATACTAAAGTGAAAGCCGCACTGAGAGAGAGAGAA

Figure 4

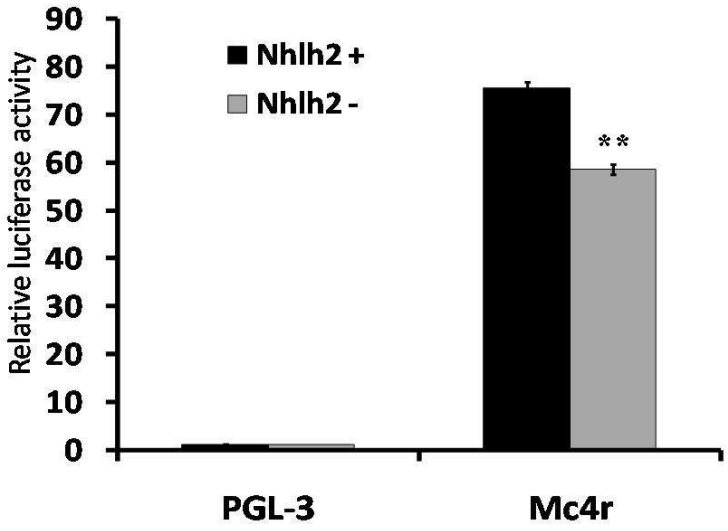
90
80
70
60
50
40
30
20
10
0
Relative luciferase activity
Nhlh2 +
Nhlh2 -
**
PGL-3
Mc4r

Figure 5

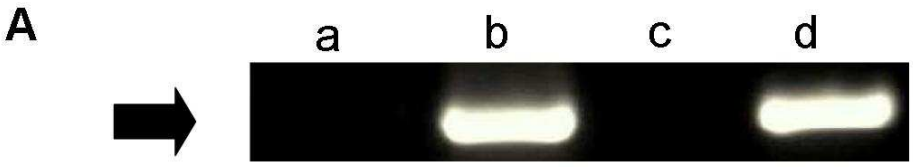
A
a
b
c
d

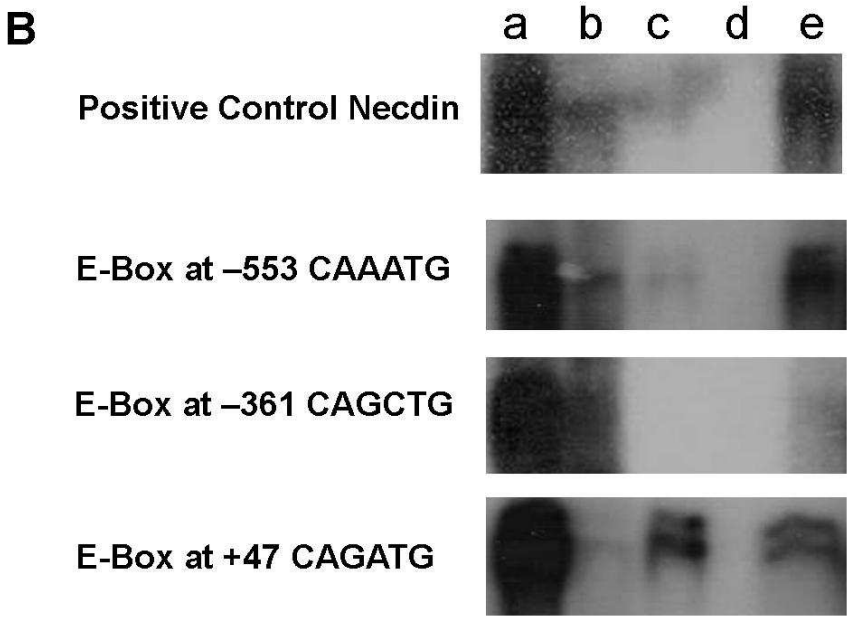
B
a b c d e
Positive Control Necdin
E-Box at –553 CAAATG
E-Box at –361 CAGCTG
E-Box at +47 CAGATG

Figure 6

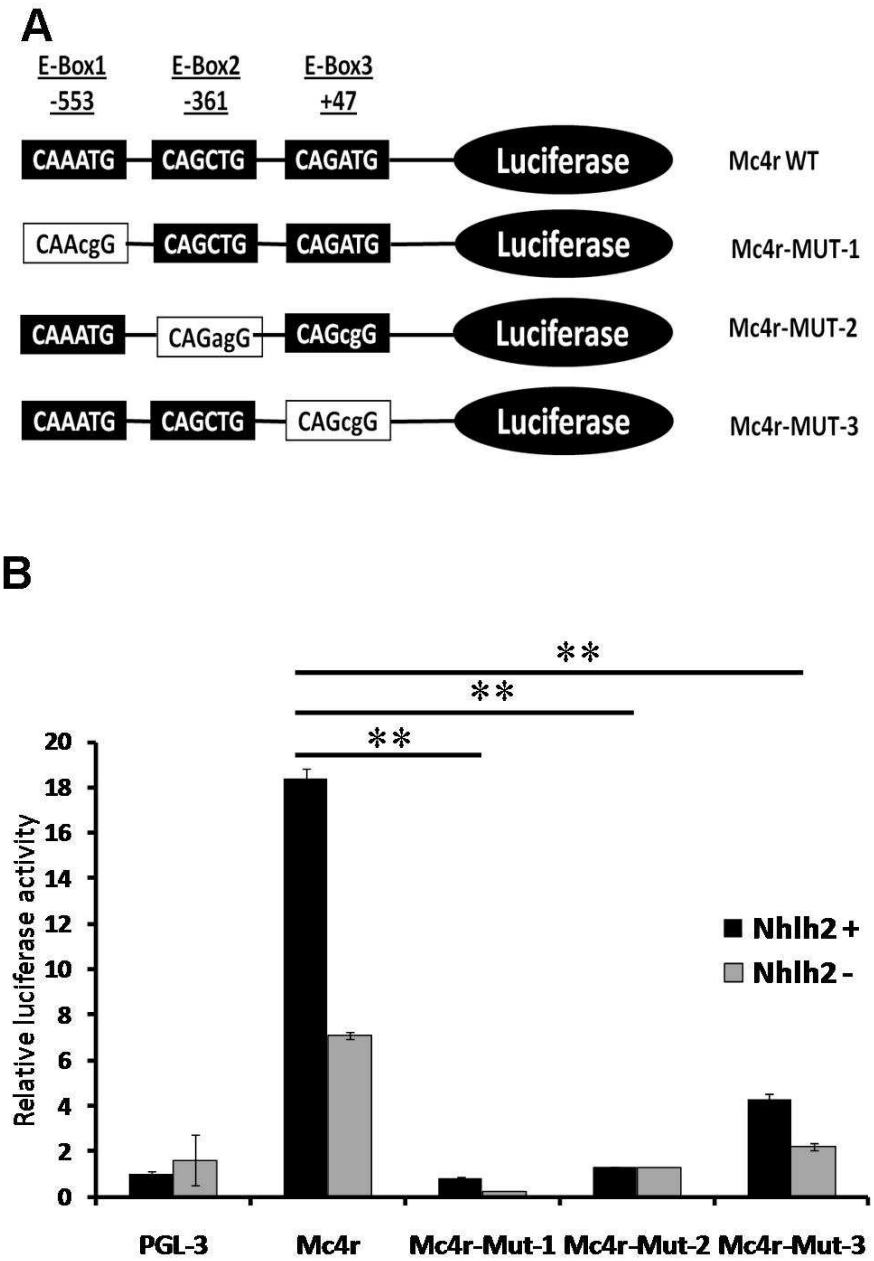
A
E-Box1
-553
E-Box2
-361
E-Box3
+47
CAAATG
CAGCTG
CAGATG
Luciferase
Mc4r WT
CAAcgG
CAGCTG
CAGATG
Luciferase
Mc4r-MUT-1
CAAATG
CAGagG
CAGcgG
Luciferase
Mc4r-MUT-2
CAAATG
CAGCTG
CAGcgG
Luciferase
Mc4r-MUT-3
B
**
**
**
Relative luciferase activity
20
18
16
14
12
10
8
6
4
2
0
Nhlh2 +
Nhlh2 -
PGL-3
Mc4r
Mc4r-Mut-1
Mc4r-Mut-2
Mc4r-Mut-3

Chapter 4

Deletion of Nhlh2 Results in Inflammation and Reduced Sympathetic Nervous System Tone in Adipose Tissue

Umesh D. Wankhade[1], Kristen R. Vella[2], Dana L. Fox[1,2], and Deborah J. Good*,[1,2]

Department of Human Nutrition, Foods and Exercise, Virginia Polytechnic Institute and State University, Blacksburg, VA 24061[1] Department of Veterinary and Animal Sciences and Molecular and Cellular Biology Graduate Program, University of Massachusetts, Amherst, MA 01002[2]

Running title: Adipose Tissue Defects in N2KO mice

Key Words: NSCL-2, HEN2, β–adrenergic receptors, uncoupling protein, torpor

Word count total: 3535

Word count abstract: 284

Author emails:

Umesh Wankhade: udvets@vt.edu

Kristen R. Vella: kvella@bidmc.harvard.edu

Dana L. Fox: Dana.Fox@Caudex.com

Deborah J. Good: goodd@vt.edu

Submitted to PLoSOne (Under review)

Introduction

The adipokine leptin is secreted by adipose tissue in proportion to fat mass to signal fat storage reserves in the body, and mediate long-term appetite controls. Since the discovery of leptin in 1994 (43), the perspective toward adipose tissue as simply a fat storage site has changed due to the recent developments in the basic understanding of adipose tissue functions. Leptin is now seen as an adipokine that signals starvation rather than energy surplus. Leptin levels drop in response to a fast, signaling the organism to eat more and decrease energy expenditure as fat storages are low (44). This is a protective mechanism developed by the body to mobilize energy stores for important physiological processes and reduce energy consuming processes that are not essential for immediate survival.

White adipose tissue (WAT) plays a major role in peripheral fatty acid synthesis and sequestration of triglycerides from normal circulation. Until recently, it was thought that the only role of brown adipose tissue (BAT) was in thermoregulation in newborns and hibernating animals. However recent studies using Positron Emission Tomography scans have shown active BAT depots in the cervical, supraclavicular, paravertebral, mediastinal, para-aortic and suprarenal regions of adult humans, suggesting that BAT contributes to energy balance in human adults as well (45-47).

Studies to date support a role for the sympathetic nervous system (SNS) as the primary initiator of adipose tissue functions in rodents (48, 49) and humans (50). For example, SNS ganglia from the thoracic and lumbar regions

have been shown to innervate fat pads (51). Increased norepinephrine turnover during conditions such as cold exposure and fasting also indicate SNS innervation of WAT (52, 53). Cold exposure and fasting also affect adipose tissue function through decreases in leptin synthesis and release (54-56). Even though injection of pseudorabies virus into inguinal WAT pads labels cells within the paraventricular nucleus of the hypothalamus, bilateral destruction of the paraventricular nucleus does not prevent WAT lipid mobilization following fasting (57). As in the majority of tissues, the SNS exerts its effects on adipose tissue through the central melanocortin system. The melanocortin system may mobilize different lipid depots in the body (50, 58-60). An injection of melanotan II, the central melanocortin receptor (Mcr) agonist, provokes a differential sympathetic drive of WAT and BAT reflected by an increased norepinephrine turnover (61). Recently, Nogueiras and colleagues showed that chemical blockage of Mc4r results in alterations in WAT metabolism and insulin sensitivity (18). Adipose tissue is innervated by Mc4r-positive SNS neurons which are ultimately responsible for regulating lipid mobilization (60, 62). Expression of both the β-adrenergic receptor (β-ARs) and uncoupling protein (UCP) family members in adipose tissue are controlled by SNS tone (63, 64). Although it is clear that the melanocortin signaling pathway plays an instrumental role in transmitting SNS signals to adipose and other tissues, the central or peripheral nature of this mediation is still unclear.

In our laboratory, we are studying nescient helix-loop-helix 2 (Nhlh2), a basic-helix-loop helix transcription factor expressed in the paraventricular and

arcuate nuclei of the hypothalamus, (10). Expression of Nhlh2 can also be found in cranial nerves (Good, unpublished) as well as the gray matter of the cervical and thoracic areas of the spinal cord (65). We have previously shown that Nhlh2 is a key component in the central melanocortin signaling pathway via transcriptional regulation of the prohormone convertase 1/3 (PC1/3) gene, especially following leptin stimulation (23). Reduced PC1/3 levels in mice containing a targeted deletion of Nhlh2 (N2KO mice) leads to lower levels of α-melanocyte-stimulating-hormone (α-MSH), the melanocortin receptor-binding neuropeptide. (10).

Considering the adult onset obesity in the mutant mice (11), the reduced melanocortinergic tone in N2KO mice (10, 23), and the expression patterns of Nhlh2 in the hypothalamus and spinal cord, we hypothesized that a targeted deletion of Nhlh2 would result in a disruption of the Mcr-SNS-Adipose tissue outflow, leading to defects in adipose tissue metabolism. The response of N2KO mice to a fasting challenge with a particular focus on WAT and BAT function was assessed in this study. The possible contribution of inflammation in WAT to the physiological changes detected in N2KO mice was explored markers of macrophages and systemic inflammation. Finally, the requirement for functional Nhlh2 in SNS inputs to WAT and BAT through expression of β-ARs and UCPs was investigated

Results

Fasting leptin levels

Ad libitum (*ad lib*) fed N2KO mice have normal food intake and leptin levels until they become overtly obese after 20 weeks of age (11). Furthermore, food intake does not differ significantly in *ad lib* fed WT and N2KO mice measured over two hours, or in mice given two hours of feeding following a 24-hour fast (66). As previously reported in pre-obese mice (35) and confirmed with these experiments, *ad lib* fed N2KO mice did not show significant differences in serum leptin levels when compared to *ad lib* fed WT mice. Interestingly, fasted N2KO mice presented a significant, 5.16-fold ($*p \leq 0.05$) increase in serum leptin levels compared to WT mice. Consistent with expected results, fasted WT mice showed reduced serum leptin levels compared to *ad lib* fed WT mice (Fig 1).

Core body temperature following fasting

Normal mice subjected to fasting, or an energy deficit, will decrease their body temperature to conserve energy. This behavior is known as torpor (67). A failure to reduce leptin can impair the ability of mice to enter torpor (68). Since N2KO mice did not reduce serum leptin levels with fasting, body temperature was analyzed as an indicator of torpor. N2KO mice have the same core body temperature as WT mice under *ad lib* feeding conditions (Fig 2), consistent with previous results (12). WT mice significantly ($*p<0.001$) dropped their body temperature approximately $3^{o}C$ during the 24 hour fast (Fig 2), as expected (69). N2KO mice only showed a $1^{o}C$ drop in body temperature with fasting (Fig 2).

This 2℃ difference between WT and N2KO mice is significantly different between the two genotypes (*p<0.001).

WAT and BAT morphology

Based on the impaired leptin response and body temperature in fasted N2KO animals, WAT and BAT morphology was examined. Hematoxylin and eosin (H&E) stained BAT from N2KO mice shows a vacuolated appearance (Fig 3A-B), while inset images shows larger lipid vacuoles in BAT From N2KO compared to the smaller vacuoles in WT. WAT from N2KO and WT mice shows an increased presence of smaller dense cells infiltrating between regions of the adipose cells in the N2KO mice (Fig 3C-D). Inset image shows individual adipocytes and adipocytes surrounded by small dense cells in N2KO mice.

Analysis of Nhlh2 expression in BAT and WAT

PCR of cDNA, using a high cycle number was carried out to determine if Nhlh2 is expressed in mRNA from either BAT or WAT. As shown in Figure 3, Nhlh2 is strongly expressed in mRNA from hypothalamus, as previously described (9, 10). However, after 40 cycles of qRT-PCR, Nhlh2 is undetectable in mRNA from BAT and WAT.

WAT Pro-inflammatory gene expression profile

Considering the altered morphology of WAT from N2KO mice, combined with the fact that Nhlh2 is not expressed in WAT, the possibility of indirect mechanisms were explored, including macrophage infiltration. RNA isolated from WT and N2KO WAT was used to measure specific inflammatory and macrophage markers. Interleukin-6 (IL-6) mRNA expression was 3.87-fold higher

in N2KO mice (Fig 4A, *p ≤0.05), indicative of an inflammatory state. WAT from N2KO mice showed a trend for higher expression levels of the macrophage markers EGF-like module-containing mucin-like hormone receptor-like 1 *(Emr1)* (1.66-fold higher) and Cluster of Differentiation 68 (*CD68)* (1.87-fold higher) in N2KO mice respectively when compared to WAT from WT mice (Fig. 5A). Consistent with increased IL-6 mRNA expression, serum IL-6 levels were also significantly increased (*p≤0.05, Fig 5B).

F4/80, macrophage specific marker protein expression in WAT

To further examine the possibility of immune cell infiltration to WAT in N2KO mice, protein expression of macrophage marker F4/80 was measured. As predicted based on the increased levels of inflammatory proteins expressed in WAT, this macrophage specific marker is easily detectable in all samples from N2KO WAT, as compared to WAT from WT mice which showed only minimal expression of the F4/80 marker (Fig 5C).

Examining SNS Input Expression Profiles In Adipose Tissue

Activation of the sympathetic nervous system is required to enter torpor as well as to initiate lipid mobilization (70, 71). Expression of β-ARs are required for a normal torpor response (72) while β-ARs and uncoupling protein (UCP) family members expression in adipose tissue are necessary for thermogenesis responses (63, 64). The expression of β-AR family members and UCPs were measured to determine if SNS input to BAT and WAT was affected in N2KO mice.

In BAT, β2–AR (**p≤0.01) and β3–AR (*p≤0.05) were significantly down-regulated in N2KO mice compared with WT mice (Fig 6A). Additionally, UCP-1 mRNA levels were significantly reduced by 4-fold in N2KO mice (**p<0.01). N2KO mice showed a reduced trend in mRNA expression levels of both β1–AR and UCP-2 compared to WT mice (Fig 6A).

In WAT, β2–AR (**p≤0.01) and β3–AR (*p≤0.05) mRNA levels were significantly down-regulated by 4-fold and 2-fold respectively in N2KO mice compared with WT mice (Fig 6B). Also, UCP-2 mRNA levels were reduced by 5.63-fold in WAT from N2KO mice compared to WT mice (**p≤0.01). Both β1–AR and UCP-2 mRNA trended toward reduced levels in N2KO mice compared to WT mice levels (Fig 6B).

Metabolic gene profile in WAT

In addition to entrance into torpor and lipid mobilization, the SNS controls important functions such as lipolysis in WAT (70, 73). The mRNA level of genes involved in lipid metabolism, such as carnitine palmitoyltransferase-1α (CPT-1α), hormone sensitive lipase (HSL), peroxisome proliferator-activated receptor-α, and δ (PPAR-α, PPAR-δ) and adiponectin, were measured. CPT-1α (*p≤0.05) and adiponectin (*p≤0.05) were down regulated in N2KO mice compared with matched WT animals. HSL, PPAR-α and PPAR-δ showed trends towards reduced expression in N2KO mice (Fig. 7).

Discussion

There are many mouse models available to study the mechanisms of obesity (74). However, only a few of these models can help elucidate the transcriptional mechanisms controlling the CNS regulation of fat metabolism. A considerable amount of work confirming the role of the SNS in neural control of adipose tissue has been conducted (48, 60, 61, 75, 76). Data presented herein shows that whole-body deletion of Nhlh2 leads to phenotypic alternations in both brown and white adipose tissue, even though Nhlh2 is not expressed in either of these tissues. We provide evidence suggesting that the hypothalamic transcription factor Nhlh2 is necessary for SNS-mediated control of BAT and WAT. Lack of Nhlh2 leads to generalized inflammation and a defective torpor response in the mutant animals.

We have repeatedly reported normal serum leptin levels in 8-week old pre-obese N2KO mice (12, 35). In order to assess conditions resulting in differential leptin levels in our pre-obese mutant animals, leptin levels in food-deprived N2KO and WT mice were determined. The normal physiological response to fasting in animals is a lowering of circulating leptin levels. However, leptin levels are elevated in fasted N2KO mice. Conditions such as fasting or cold exposure normally stimulate WAT's sympathetic drive and decreases leptin synthesis/release in mice (52, 53), reducing leptin expression in isolated adipocytes (77). These processes are necessary conditions for torpor to occur (68). We have previously reported that N2KO mice also do not reduce circulating

leptin levels following 24-hour exposure to cold (35). Taken together, these data suggest that N2KO mice have a defective torpor response.

To further explore the defective torpor phenotype in N2KO mice, we examined the expression of β-ARs. β-ARs are expressed predominantly in adipose tissues (78-82), and are required for fasting-induced torpor in mice, as β3-AR antagonists block a normal torpor response (68, 72). Here, we report that N2KO mice express β2–AR and β3–AR mRNA at significantly lower levels in both BAT and WAT indicating lowered SNS input from the CNS. This is consistent with earlier findings that N2KO mice have severely reduced innervation of WAT including sensory and autonomic nerves (71). Although β3-AR knockout mice develop obesity at an early age (3 weeks), this is without hyperphagia, which is similar to N2KO mice and suggests an impairment of energy expenditure, rather than energy intake pathways (11, 83, 84).

The aberrant adipose phenotype of N2KO mice includes morphological tissue changes. BAT from N2KO mice appears packed with larger lipid vacuoles compared with the dense, small lipid vacuoles in BAT from WT mice. This appearance is similar to that shown by Bachman and colleagues for β1–β3-AR double knockout mice, although the authors of this paper state that the BAT appears normal (85). Furthermore, in N2KO mice, WAT histology indicates the presence of smaller dense cells infiltrating between the adipose cells. Evidence of slightly higher levels of macrophage-specific markers, as well as significantly increased levels of serum IL-6 and mRNA, suggest an inflammatory state for N2KO WAT. Our results are consistent with the reduced peripheral innervation

and vascularization of adipose tissue in N2KO mice previously shown to lead to preadipocyte and macrophage infiltration to WAT and changes in tissue architecture (71).

SNS controls many adipose tissue functions including lipolysis and lipogenesis, and reduced innervation leads to reduced lipolysis and increased lipogensis (48, 61, 70). In the present study, reduced mRNA expression of CPT1-α and HSL is indicative of reduced lipolysis. Likewise, the reduction of adiponectin, PPAR-α and PPAR-δ gene expression contributes to our contention that the adipose tissue from N2KO mice has abnormal functionality. Adiponectin levels are inversely related increased IL-6 levels as reported earlier (86). Considering the inflammatory state of WAT in N2KO, reduced adiponectin levels are consistent with previous literature (86).

In summary, these results support a role for Nhlh2 in the maintenance of SNS tone ultimately affecting adipose tissue. Loss of SNS tone leads to systemic inflammation, altered morphology of adipose tissue, and aberrant expression of uncoupling proteins in these tissues. These results provide an explanation for the abnormal leptin response and failure of torpor induction following both fasting and cold exposure. As Nhlh2 is not expressed in WAT or BAT the transcriptional activity by Nhhl2 within the CNS is proposed to affect the peripheral adipose-specific metabolic response. Furthermore, we have previously shown that Nhlh2 transcriptionally regulates expression of the neuropeptide processing enzyme PC1/3, leading to reduced expression of melanocortins throughout the hypothalamus. As the melanocortin signaling pathway has been

implicated in SNS tone and WAT metabolism, our studies suggest a link between transcriptional regulation of melanocortin pathway genes by Nhlh2 and downstream peripheral effects leading to abnormal adipose functioning.

Materials and Methods

Animals

All animal protocols were approved by the Institutional Animal Care and Use Committee at Virginia Polytechnic Institute and State University, or the University of Massachusetts-Amherst (leptin measurements, body temperature and adipose histology). Animal colony maintenance, breeding and genotyping have been previously described (10). N2KO and WT mice were maintained in 12 hr light, 12 hr dark conditions with *ad libitum* (ad lib) access to food (4.5% crude fat). At 14 weeks all mice were euthanized by CO_2 asphyxiation at 1300 hr to standardize hormone and steroid levels that fluctuate hourly. For the fasting studies male WT and N2KO mice were individually housed in hanging wire-bottom cages and given free access to food and water for 48 hours prior to the start of the experiment. All experiments began at 11 AM on the day of testing (day 1). Animals with *ad lib* food received a measured amount of approximately 30 grams of food. All other animals began a 24 hour fast until 11 AM the following day. At 11 AM on day 2, body temperature was measured using a Thermalert TH-5 mouse rectal probe attached to a Physitemp (Clifton, NJ) digital thermometer. All mice are euthanized by 1 PM. Blood was collected by exsanguination and serum was used for leptin and Il-6 assays (below).

Histology

WT and N2KO mice were euthanized under *ad libitum* conditions. Brown adipose tissue (BAT) was isolated by dissecting the interscapular brown fat depot. White adipose tissue was dissected by removing the visceral intra-

abdominal fat pad from mice. Tissue was fixed overnight in the tissue fixative Histochoice (Amresco, Solon, OH) and then embedded in paraffin blocks at the Pioneer Valley Life Sciences Institute (Springfield, MA) or at the AML Laboratories Inc. (Rosedale MD). 6μm sections were placed on glass slides (VWR Superfrost Plus, West Chester, PA). After staining with Hematoxylin and Eosin, slides were cover-slipped. Slides were examined under an Olympus BH-2 microscope (Olympus, Melville, NY) with the same exposure time, brightness and contrast for comparison groups. 40X and 10X images were taken. For both BAT and WAT adipose tissue, N = 3 WT and N = 3 N2KO mice examined.

qRT-PCR from white and brown adipose tissue to detect gene expression

Intra-abdominal visceral WAT was collected from WT (N = 7) and N2KO (N = 11) 14-weeks old mice. Intrascapular BAT was collected from WT (N=6) and N2KO (N=7)) 14-weeks old mice. Tissues were homogenized into 4 M guanidine isothiocyanate buffer. Samples were layered over 5.7 M cesium chloride buffer and spun for 18 h at 120,000 X *g* at 20^0 C. The supernatant was discarded, and RNA was resuspended in water and stored frozen until use. RNA was then DNAse treated prior to cDNA preparation. cDNA was created using reverse transcriptase in a magnesium buffer (Promega Corp.) for 1 hr at 42^0 C. qRT-PCR was performed using *Power* SYBR® Green, PCR master mix (2X). mRNA levels of each gene of interest was normalized against β-actin. A list of primer sequences used for amplification is found in Table 1. β–actin levels are constant between WT and N2KO animals in all energy states (9). Normalized levels of mRNA were measured in triplicate per individual mouse from which sample

means were calculated for each mouse. Data is presented as the fold-difference relative to the WT control group. For each mRNA amplified, melting-curve analysis was done to confirm the presence of a single amplicon.

Western blot of white adipose tissue to detect F4/80 protein expression

For F4/80 protein analysis, abdominal adipose tissue was collected (N= 3 WT and N=4 N2KO) in RIPA buffer, homogenized and processed for Western analysis using the published methods (87). Equal amounts of protein (20 μg/lane), as determined using BCA Protein Assay (Pierce, Thermo Scientific, Rockford, IL) was run on a 8% SDS polyacrylamide gel and transferred to nitrocellulose membrane. Western blotting was performed using a rat monoclonal F4/80 antibody (Abcam, Cambridge, MA) with rabbit anti-rat HRP linked antibody as a secondary antibody. Chemoluminescent signal (ECL, Pierce, Rockford, IL) was detected.

Serum protein measurements

Serum leptin was measured using the mouse leptin ELISA (Quantikine M Mouse Leptin immunoassay, R&D 30 Systems, Minneapolis, MN) on trunk blood collected from *ad libitum* fed (N = 6, each genotype) or 24-hour fasted (N = 5, each genotype) mice. Serum IL-6 levels were measured by ELISA (Mouse IL-6 Ready-SET-Go! ELISA Kit, eBiosciences, Inc. San Diego, CA) in serum separated from the blood collected from *ad libitum* fed mice WT (N=7) and N2KO (N=11).

Non-quantitative Polymerase Chain Reaction

RNA was isolated from WAT, hypothalamus and BAT by guanidine isothiocyanate preparation. cDNA was created using reverse transcriptase in a magnesium buffer (Promega Corp.) for 1 hr at 42^0 C, and DNAse-treated prior to amplification. PCR was performed on 2μl of DNAse-treated cDNA, or mouse genomic DNA (control) in a 25 μl reaction volume using Taq DNA Polymerase (Qiagen, Valencia, CA) and gene specific oligonucleotide primers (TABLE 1). Forty cycles of 1 min at 94^0C, 1 min at 57^0C and 1 min at 72^0C with the extension time of 10 min at 72^0C was performed to amplify.

Statistical analysis

All values are expressed as mean ± SEM unless indicated otherwise. Comparison of means between two groups was made using unpaired two-tailed Student's T-test. Significance is expressed at *$p \leq 0.05$; **$p \leq 0.01$.

Author Contributions

Conceived and designed the experiments: UW, KRV, DLF, DJG. Performed the experiments: UW, KRV, DLF. Analyzed the data: UW, KRV, DLF, DJG. Wrote the paper: UW, KRV, DLF, DJG**.**

Acknowledgments

The authors would like to thank Alison Bardwell, Christopher Coyle, Risa Pesapane, Haiyan Zhang and Joanna Jacob for excellent technical assistance.

This work was supported by funding from the NIH: R01 DK59903 (to DJG) and T32 MH47538 (to KRV) and internal departmental and college funds (DJG). The authors declare that there is no conflict of interest that would prejudice the impartiality of this scientific work.

Figure Legends

Fig. 1 Serum leptin levels in *ad lib* fed and fasted WT and N2KO mice

Serum leptin was measured in WT and N2KO mice following *ad libitum* feeding (*Ad lib*), and following a 24 hour fast (Deprived). Data are reported as leptin concentration (pg/ml) ± SEM. (*$p \leq 0.05$).

Fig. 2 Core body temperature in *ad lib* fed and fasted WT and N2KO mice

Body temperature (^{o}C) was measured using a rectal thermometer in WT and N2KO mice following *ad libitum* feeding (*Ab lib*) and following a 24-hour fast (**$p \leq 0.01$).

Fig. 3 Histological analysis of Brown and White Adipose Tissues from N2KO and WT mice

H&E staining of Brown Adipose Tissue (**A**) or White Adipose Tissue (**C)** from WT, (**B)** and **(D)** from N2KO. Scale bars for whole and inset pictures are given.

Fig. 4 Nhlh2 expression WAT, Hypothalamus and BAT

Ethidium bromide-stained agarose gel showing PCR results following a 40-cycle amplification of mouse genomic DNA (control) or RNA from white adipose (WAT), hypothalamus (Brain) and brown adipose (BAT).

Fig. 5 Expression profile for pro-inflammatory genes from WT and N2KO mice

A. Relative quantitative expression in RNA from WAT isolated from ad lib fed WT and N2KO for interleukin-6 (IL-6), Cluster of Differentiation 68 (CD68) and EGF-

like module-containing mucin-like hormone receptor-like 1 (Emr1). The data are reported as mean expression level relative to WT expression ±SEM. (*p ≤ 0.05). **B**. Serum IL-6 levels were measured from ad lib fed WT and N2KO mice. The data is reported as the serum level (pg/ml) ±SEM (*p≤0.05).

C. Western analysis of WAT for F4/80 expression in protein extracted from ad lib fed mice. Equal total protein amounts were added for N=3 WT mice, and N=4 N2KO mice.

Fig. 6 Expression profile for genes regulated by SNS input to BAT and WAT

Relative quantitative expression levels for β–adrenergic receptors (β1AR, β2AR and β3AR) and uncoupling proteins (UCP1 and UCP2) in RNA isolated from BAT (**A.**) and WAT (**B.**). The data is reported as the mean expression level relative to WT expression ± SEM. (*p≤0.05, **p≤0.01).

Fig. 6 WAT metabolic gene expression profile in WT and N2KO mice

Relative quantitative expression levels of carnitine palmitoyltransferase-1α (CPT-1α), Adiponectin, hormone sensitive lipase (HSL), and peroxisome proliferator-activated receptor alpha (PPARα) and delta (PPARδ) in WAT from ad lib fed WT and N2KO. All samples were normalized to β-actin expression. The data is reported as the mean expression level relative to WT expression ±SEM. (*p≤0.05, **p≤0.01).

Table 1: Primer sequences used for quantitative real-time RT-PCR assays
All sequences are to the mouse genes, and the forward and reverse primers are indicated.

Gene	Direction	Oligonucleotide sequence 5'--3'
Adiponectin	Forward	TGTTCCTCTTAATCCTGCCCA
	Reverse	CCAACCTGCACAAGTTCCCTT
β-actin	Forward	GGAATCCTGTGGCATCCAT
	Reverse	GGAGGAGCAATGATCTTGATCT
β1-AR	Forward	GCTGCAGACGCTCACCA
	Reverse	GCGAGGTAGCGGTCCAG
β2-AR	Forward	CACAGCCATTGCCAAGTTCG
	Reverse	CGGGCCTTATTCTTGGTCAGC
β3-AR	Forward	AGACAGCCTCAAATGCATCC
	Reverse	CCCAGTCCACACACCTTTCT
CD68	Forward	CACCACCAGTCATGGGAATG
	Reverse	AAGCCCCACTTTAGCTTTACC
CPT-1α	Forward	AAAGATCAATCGGACCCTAGACA
	Reverse	CAGCGAGTAGCGCATAGTCA
Emr1	Forward	TTGTACGTGCAACTCAGGACT
	Reverse	GATCCCAGAGTGTTGATGCAA
HSL-1	Forward	CCTCATGGCTCAACTCC
	Reverse	GGTTCTTGACTATGGGTGA
Nhlh-2	Forward	CAGTTGGCGTGAAGAGGTAGA
	Reverse	AATGCCCACGAGAAATACCA
PPAR- α	Forward	TGGGGATGAAGAGGGCTGAG
	Reverse	GGGGACTGCCGTTGTCTG
PPAR-δ	Forward	ACAGTGACCTGGCGCTCTTC
	Reverse	TGGTGTCCTGGATGGCTTCT
UCP-1	Forward	AAACAGAAGGATTGCCGAAA
	Reverse	TGCATTCTGACCTTCACGAC
UCP-2	Forward	CTACAAGACCATTGCACGAGAGG
	Reverse	AGCTGCTCATAGGTGACAAACAT

Figure 1

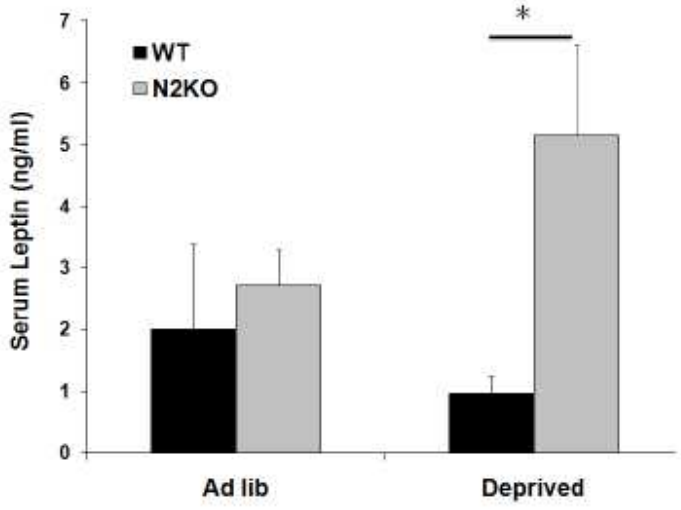

Figure 3

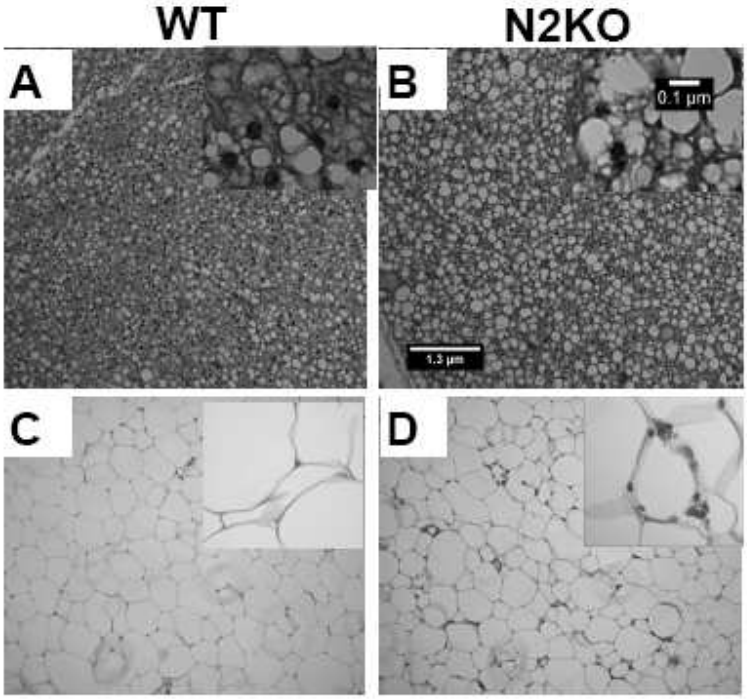

Figure 4

Figure 5

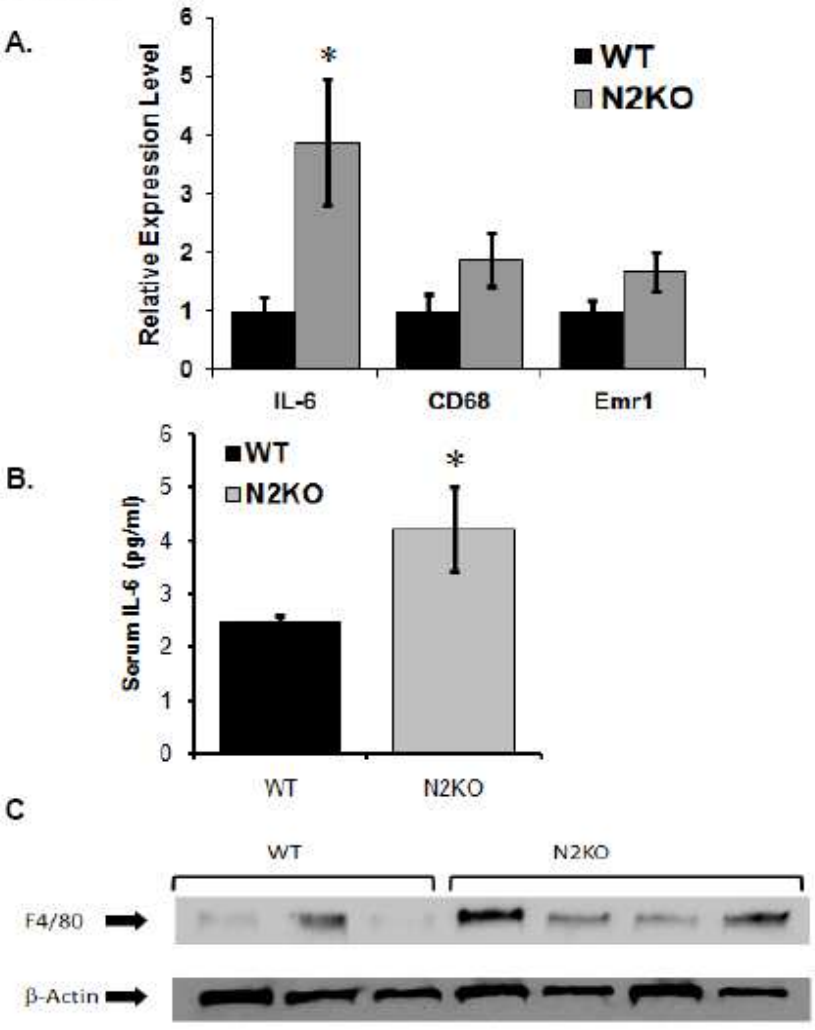
A.
Relative Expression Level
6
5
4
3
2
1
0
*
WT
N2KO
IL-6
CD68
Emr1
B.
Serum IL-6 (pg/ml)
6
5
4
3
2
1
0
WT
N2KO
*
WT
N2KO
C
WT
N2KO
F4/80
β-Actin

Figure 6

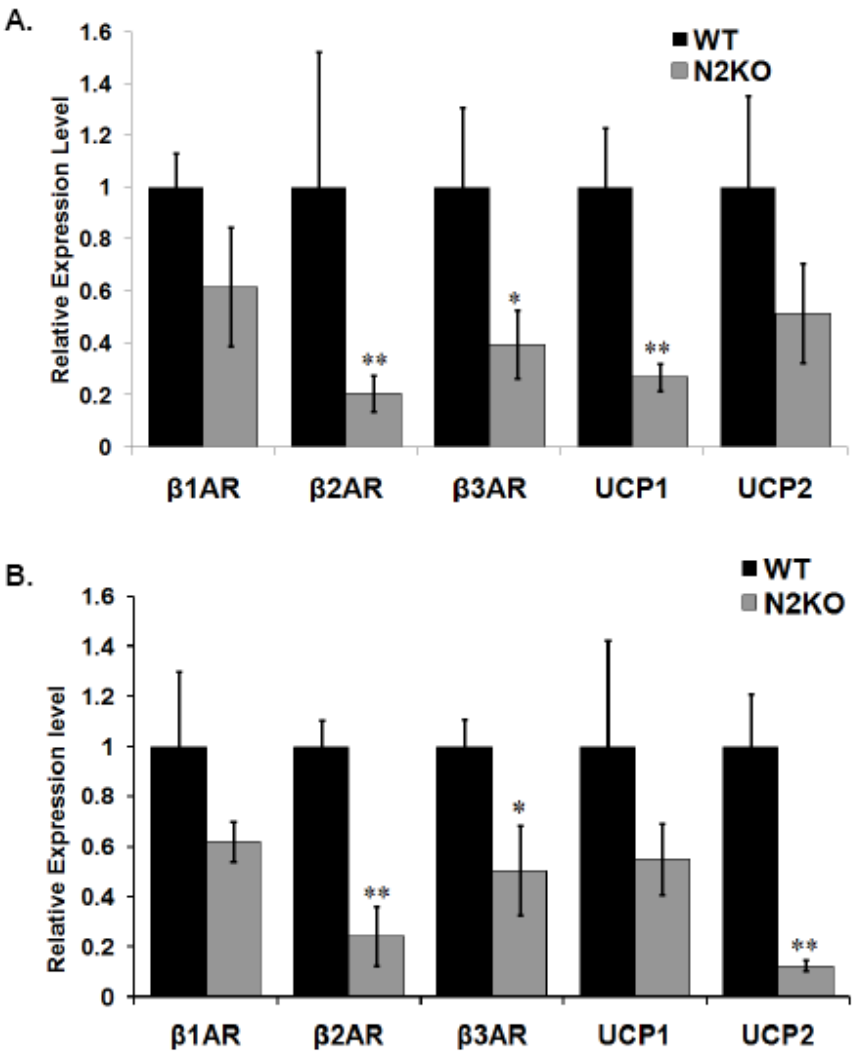
A.
WT
N2KO
Relative Expression Level
1.6
1.4
1.2
1
0.8
0.6
0.4
0.2
0
**
*
**
β1AR
β2AR
β3AR
UCP1
UCP2
B.
WT
N2KO
Relative Expression level
1.6
1.4
1.2
1
0.8
0.6
0.4
0.2
0
**
*
**
β1AR
β2AR
β3AR
UCP1
UCP2

Figure 7

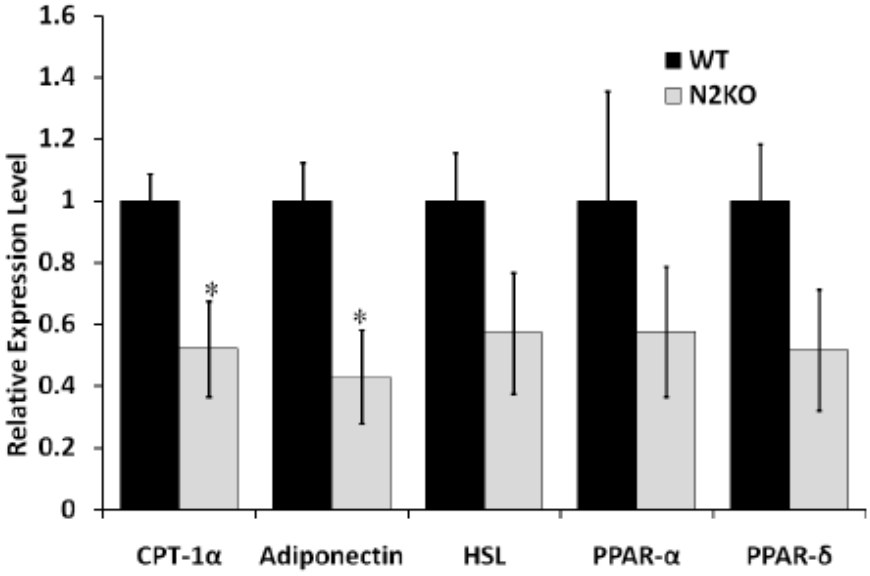
1.6
1.4
1.2
1
0.8
0.6
0.4
0.2
0
Relative Expression Level
WT
N2KO
*
*
CPT-1α
Adiponectin
HSL
PPAR-α
PPAR-δ

Chapter 5

Effect of targeted deletion of Nescient Helix-Loop-Helix 2 on peripheral fatty acid metabolism in skeletal muscle and liver

Umesh D. Wankhade, Ryan McMillan, Aaron Rudd, Matthew W. Hulver and Deborah J. Good

Department of Human Nutrition, Foods and Exercise, Virginia Polytechnic Institute and State University, Blacksburg, VA 24061

Running title: Characterization of N2KO phenotype

Key Words: NSCL-2, HEN2, Fatty Acid Oxidation, Obesity, Glucose Homeostasis

Introduction

Mutations/polymorphisms in genes of the melanocortin pathway are one of the most common genetic associations with obesity in humans (88, 89). Both human and mouse studies have contributed to our understanding of melanocortin signaling pathways in the hypothalamus and its role in energy metabolism (89). Mainly, melanocortin receptors such as melanocortin 4 receptor (Mc4r) and Mc3r sense satiety/anorexigenic signals in the CNS to fed or fasted states, and mediate its effects to regulate food intake and energy expenditure. Melanocortin transmits its effects through ligands, i.e. α-Melanocyte Stimulating hormone (α-MSH). Ligands such as α-MSH are generated by posttranslational processing of proopiomelanocortins (POMC) by enzymes such as prohormone convertases (PC1/3 and PC2) and other peptidases. The crucial importance of the melanocortin pathway to energy homeostasis is evident from the obesity developed in animals or humans that have mutation(s)/ polymorphism(s) in alleles of POMC, MC4R, MC3R and the related neuropeptide processing enzymes such as PC1/3 and PC2 (88, 90-92). Within the melanocortin pathway, to date, polymorphisms in MC4R are one of the most frequent genetic causes responsible for obesity in humans (93).

While it is clear that the melanocortin signaling pathway is fundamental to the regulation of body weight, there is still much to be done to understand the upstream and downstream effectors and regulators of this essential pathway. We have previously shown that the basic helix-loop helix transcription factor, nescient helix-loop-helix 2 (Nhlh2) is a key component in the melanocortin

signaling pathway. Targeted deletion of Nhlh2 in mice (N2KO mice) results in adult-onset obesity characterized by reduced physical activity (12). Nhlh2 is required for transcriptional regulation of the PC1/3 gene, especially following leptin stimulation [16, 17]. Reduced PC1/3 levels in N2KO mice lead to lower levels of the melanocortin neuropeptide, α-MSH (10). Nhlh2 also transcriptionally regulates the α-MSH receptor, Mc4r through three E-box motifs on the Mc4R promoter (Wankhade et al., in preparation). Thus, targeted deletion of Nhlh2 leads to impairment of the melanocortin pathway through regulation of at least two distinct genes.

Adult onset obesity in N2KO in mice occurs in the absence of hyperphagia, which suggests the impairment of energy expenditure rather than intake. Reduced voluntary physical activity in N2KO mice leads to reduced voluntary energy expenditure in these mice, but metabolic changes in the animal could contribute to reductions of physiological energy expenditure as well. In the present study, we explore the energy expenditure pattern of N2KO mice, compared to WT mice. Analysis of glucose homeostasis, fatty acid oxidation, and gene expression patterns for liver and skeletal muscle were conducted to understand the N2KO mouse phenotype, with respect to peripheral energy metabolism.

Results

Body weight and composition of N2KO mice

Literature published by our laboratory earlier has shown that N2KO mice develop adult onset obesity with reductions in voluntary physical activity (11, 12). Findings from the present study are consistent with these previous data because there were no differences in body weight between two genotypes at the age of 11 weeks (TABLE 1), although there was a slight trend towards the N2KO animals weighing more. These body weights represent pre-obese state of this adult-onset obese model. However, MRI scans shows differences in their body composition. N2KO mice had higher percentage of body fat compared to their WT counterparts (TABLE 1). Lean body weight did not differ between the two genotypes.

Insulin and glucose homeostasis

Deletion of Nhlh2 results in a 40-60% reduced expression of the neuropeptide processing enzyme PC1/3 and reduced levels of α-MSH neuropeptide (10, 94). Because Mc4rKO mice exhibit impaired glucose homeostasis (95), glucose and insulin tolerance were assessed in N2KO mice. Food deprived N2KO mice exhibited a glucose tolerance similar to WT mice with a 2 gm/kg body weight glucose challenge (Figure 1A). N2KO mice were significantly compromised in their ability to normalize blood glucose level following insulin injection with an elevated glucose reading throughout the challenge (Figure 1B).

Fatty acid oxidation

Considering N2KO's high body fat content and their impaired glucose homeostasis, fatty acid oxidation patterns were studied in the mutant animals. Fatty acid metabolism was measured in whole homogenates from dissected red and white fibers isolated from both quadriceps. In red fibers of quadriceps muscle, N2KO mice showed high rates of fatty acid oxidation compared to WT animals (Figure 3A) (CO_2 production $p<0.05$, for acid soluble metabolites $p<0.1$ and total $p<0.02$). Neither white quadriceps nor liver showed any significant differences between the two genotypes (Figure 3B and 3C).

Energy expenditure

To determine N2KO's energy expenditure pattern and preferred source of substrate for energy, indirect calorimetry was performed. Respiratory exchange ratio (RER) of WT followed the normal circadian pattern, i.e. during the dark phase there was a high RER and during the light phase, a lower RER. However, N2KO mice were more active during the light phase with a higher RER than in the dark phase where RER was low (Figure 3A). Overall, during the dark phase, the RER of the N2KO mice was significantly lower than WT (RER, WT =0.85±0.03, N2KO=0.77±0.03 *$p \leq 0.05$), whereas during the light phase there was no difference (Figure 3B).

Skeletal muscle gene expression

Increased body fat, impaired glucose tolerance and high fatty acid oxidation in the mutant animals prompted additional detailed investigation of the expression of skeletal muscle genes involved in fatty acid oxidation. In N2KO

mice, two of the four genes responsible for lipogenesis (Figure 4A) showed overall increased mRNA expression compared to their WT counterparts. Stearoyl-CoA desaturase (SCD) and Sterol Regulatory Element Binding Proteins-1c (SREBP1c) were both significantly upregulated (*p≤ 0.05), while Fatty acid synthase (FAS) and Acyl Co-A Carboxylase-α (ACC-α) were unchanged. Lipolytic genes such as hormone sensitive lipase (HSL) and lipoprotein lipase (LPL) were also examined. Consistent with the high fatty acid oxidation rates in skeletal muscle, HSL showed increased expression in N2KO (*p≤ 0.05), whereas LPL was unchanged. The expression of peroxisome proliferator activated receptors and their coactivators were also studied, because of the role they play in lipid and energy metabolism. PPAR-δ was significantly upregulated in N2KO (*p≤0.05), whereas PPAR-α and PPAR-γ as well as the coactivators PGC1-α and PGC1-β were unchanged.

Liver gene expression

To get a better understanding of fatty acid metabolism in other tissues, we studied gene expression in liver. SCD mRNA expression was significantly higher in N2KO compared to WT (*p≤0.05), whereas LPL, FAS, ACC-α and SREBP1c were unchanged (Figure 5A). The PPARs and their co-activators were also studied. Expression of PPAR-α and PGC1-β mRNA were both significantly higher in N2KO as compared to their WT counterpart (*p≤ 0.05) (Figure 5B). However, PPAR-δ and PPAR-γ and PGC1-α were unchanged (Figure 5B).

Discussion

The contribution of genetics to the epidemic of obesity is significant. Continuous scientific efforts to study the mechanisms of the genetic origins of obesity at the molecular and physiological level are ongoing. Some of the mouse models developed have provided excellent tools to explore the underpinnings of obesity. N2KO, as a mouse model has its own importance. Since early studies in 1997, when it was first identified that N2KO mice develops hypogonadism and obesity, there has been huge addition of understandings to the role of Nhlh2 in body weight and reproductive regulation (9-12, 23, 41, 71, 96, 97). As a transcription factor, Nhlh2 regulates the transcription of important genes in the melanocortin pathway, including PC1/3 and Mc4r (Wankhade et al., manuscript in preparation) (23). Both of these genes are linked as causes of human monogenetic obesity (98-101). Nhlh2 has also been linked to human obesity (Good and Bowden, unpublished). In the present study, further understanding of the role of Nhlh2 in peripheral energy availability mechanisms is provided, specifically implicating Nhlh2 in control of whole body energy expenditure pathways. The main objective of this study was to explore the effects of the deletion of Nhlh2 on peripheral energy expenditure, glucose homeostasis and fatty acid oxidation. As Nhlh2 is already established as a key transcriptional regulator in the melanocortin pathway, this study provides an opportunity to identify the peripheral effects of impaired transcriptional regulation of two key melanocortin pathway genes, Mc4r and PC1/3 (23). Earlier, it has been shown that the N2KO mouse develops adult onset obesity due to reduced voluntary

physical activity, surprisingly in the absence of hyperphagia (12). Normal food intake suggests that the energy intake contributions of total body energy equilibrium are undisturbed in the N2KO mice; however energy expenditure is impaired. In the present study, body composition, glucose homeostasis, fatty acid oxidation pattern and mRNA profiling of skeletal muscle and liver were analyzed.

Adult onset obesity in N2KO has been reported (12). In this study, while there was no difference in the body weight of N2KO and WT at the age of 12 weeks, there is difference between the fat content between the two genotypes. In the present study, N2KO mice had a significantly higher body fat content than WT at 12 weeks of age. In an earlier study, body composition analysis was conducted using the oven drying method (102), whereas in the present experiment, MRI was used to estimate the fat and fat free weight. The oven drying method calculates body fat mathematically by considering the water content of the body. Carcass weight is weighed separately consisting of brain, intestine, and the eviscerated body which makes body composition analysis more prone to errors by oven baking method. Whereas, the method we used during the present study is based on a magnetic resonance imaging technique, it calculates body fat, lean mass and water content based on the body weight on unanesthetized animal. For these reasons we suspect that the sensitivity of the MRI is higher than the oven drying method.

N2KO mice were assessed for glucose homeostasis, as glucose regulation by peripheral tissues is an important component of energy expenditure. Although, there were no significant differences in N2KO and WT for

glucose tolerance overall, N2KO mice have a slightly higher fasting glucose and their clearance of glucose after a glucose challenge appears to be later and slower compared to WT mice. Impaired insulin responses are also present in N2KO mice. These animals are not able to provoke the same kind of response as WT mice, suggesting that insulin sensitivity is significantly reduced in N2KOs compared to WT. These data are in line with mouse models containing deletions of genes in the melanocortin pathway, as Mc4rKO mice do not develop glucose intolerance and insulin resistant status until they are challenged with high fat feeding (95). Likewise, both PC2 and PC1/3 mutant mice maintain normal glucose tolerance in response to glucose injection, but do exhibit hyperinsulinemia (103, 104). N2KO mice also require high insulin which is evident by their lowered insulin sensitivity to maintain normal glucose tolerance where they are struggling to maintain the normal glucose levels after injection of glucose in GTT. The N2KO mice were maintained on 4.5% standard chow diet, which may be one of the reasons why glucose tolerance level has not deteriorated as it did in the Mc4rKO mice.

In earlier studies, the absence of hyperphagia accompanied by a progression towards adult onset obesity led to questions about the energy expenditure capacity of N2KO mice. To understand N2KO's preferred source of energy, fatty acid oxidation and indirect calorimetry were conducted. Surprisingly, the rate of fatty acid oxidation in red muscle fibers from N2KO mice was higher than age- and sex-matched WTs, whereas white muscle fibers and liver showed no differences between genotypes. Furthermore, and supportive of this finding,

the RER of N2KO mice was in the range of 0.77 to 0.79 and significantly lower than the comparable RER measurements of WT's, which ranged from 0.81 to 0.85. The lower RER measurement in N2KO mice suggests that the preferential source of energy is fat and carbohydrate, whereas in WT mice, a mix of carbohydrates and fats are used as a source of energy. Increased fatty acid oxidation in skeletal muscle in N2KO is thus reflected in lower RER.

Further complimenting these findings, gene expression profiles of skeletal muscle corroborated the lower RER and higher fatty acid oxidation rate in N2KO mice. In particular, high body fat content, higher fatty acid oxidation and lower RER values in N2KO imply that there may be altered nutrient partitioning, with N2KO mice preferring fat as a source of energy. Lipogenic genes such as SCD and SREBP1c, as well as lipolytic genes such as HSL all have significantly higher expression in N2KO compared to WT mice. Increased fatty acid oxidation, accompanied by increased expression of genes involved in lipid metabolism, suggests that a high turnover of lipids is occurring in skeletal muscle. Cardiac muscle of *ob/ob* mice have been reported to have a high rate of fatty acid oxidation in spite of their highly insulin resistant-glucose intolerant status (105). Increased lipogenic genes expression in skeletal muscle as well as liver suggests an overall higher fatty acid synthesis in N2KO mice, which is consistent with the fact that they have higher fat % than WT mice.

Increased PPAR-δ in skeletal muscle, and PPAR-α and PGC1-β expression in liver suggest a high rate of lipid turnover in these tissues, as PPAR-δ and PPAR-α regulates the oxidative processes, whereas PGC1-β has

been reported to play role in fatty acid synthesis (106, 107). Higher PPAR-δ has been associated with increased fatty acid oxidation (108) which is consistent with the higher fatty acid oxidation in skeletal muscle. The role of PPARs in fatty acid oxidation and glucose homeostasis in N2KO is still speculative and detailed exploration needs to be undertaken to make any conclusion.

Earlier, we reported that Nhlh2 controls transcription of several key genes in the melanocortin pathway (Wankhade et al., in preparation and (23)) and that N2KO mice have a reduced α-MSH production. Reduced MSH secretion and Mc4r signaling have been associated with increased weight gain and insulin sensitivity in humans (109, 110). In addition, the role of central nervous system and melanocortin pathway's (CNS-Mcr) role in energy expenditure and glucose metabolism is well documented (18, 95). Recently, Nogueiras et al. has reported that lipid metabolism is also controlled by the CNS-Mcr pathway (18). As Nhlh2 is a transcriptional regulator of both PC1/3 and Mc4r (Wankhade et al., in preparation) (23), the absence of Nhlh2 in N2KO mice may impair melanocortin pathway signaling and lead to reduced melanocortinergic tone in peripheral tissues. This reduced melanocortinergic tone is one of the explanations for impaired glucose homeostasis and energy expenditure pattern in N2KO.

Data presented herein, suggests that N2KO mice uses fat as an energy substrate and store carbohydrate in the form of fat, as evidenced by increased lipogenic gene expression in both liver and skeletal muscle. Results presented herein shed new light on the whole-body phenotype of adult onset obesity in

N2KO mice, linking transcriptional regulation in the brain to downstream effects on tissue-specific and whole-body metabolism.

Material and methods

Animals

All animal protocols were approved by the Institutional Animal Care and Use Committee at Virginia Polytechnic Institute and State University. Animal colony maintenance, breeding and genotyping have been previously described (10). N2KO and WT mice were maintained in 12 hr light, 12 hr dark conditions with *ad libitum* (ad lib) access to food (4.5% crude fat) and water. At 12-14 weeks all mice were euthanized by CO_2 asphyxiation. Body weight and body composition were obtained the day before sacrifice. Body composition was determined by using the Minispec LF50 (Bruker Optics, Billerica, MA), an NMR analyzer for whole body composition assay of live, unanesthetized mice. Animals were sacked at 11-14 weeks of age. Red and white quadriceps was collected for fatty acid oxidation study. Gastrocnemius separated from soleus muscle was collected in GIT for RNA isolation. Liver was collected in GIT to isolate RNA.

Glucose and Insulin Tolerance Assay

Mice were fasted for 12 hr and bled through the caudal vein for assessment of fasting blood glucose (FBG) concentrations using FreeStyle FREEDOM-*lite*® Glucometer (Abbott Diabetes Care Inc.). Mice were then injected intraperitoneally with glucose (D-Glucose [Sigma-Aldrich, USA]; 2 gm/kg body weight) and or insulin (Insulin [Elli-Lily Corp. Indianapolis, USA]; 0.75 U/kg body weight), with determination of glucose levels at 15, 30, 90, 120 and 180 min (glucose tolerance) and 15, 30, 60, 90 min (insulin tolerance) post challenge.

Fatty acid oxidation in skeletal muscle and liver

Fatty acid metabolism in freshly isolated liver and skeletal muscle was studied. Fresh skeletal muscle separated into red and white fibers and liver was collected from WT and N2KO mice (WT n=9 and N2KO N=7), minced and homogenized in modified sucrose-EDTA medium and then homogenates was incubated with [1-^{14}C] palmitic acid (NEN, Boston, MA) for measures of fatty acid metabolism. Rate of fatty oxidation was measured by production of ^{14}C-labeled acid-soluble metabolites, which is measure of the tricarboxylic acid (TCA) cycle intermediates and acetyl esters representing incomplete oxidation and [^{14}C]CO2 states complete oxidation. Reaction was stopped by addition of 100 ul of 4N sulfuric acid after one hr incubation at 37^{0}C. CO_2 produced was trapped in 1N sodium hydroxide. Scintillation counter was used to measure CO2 and acid soluble metabolites (27, 28).

Indirect calorimetry

Set of mice (WT N=9, N2KO N=7, all male) at the age of 8-10 week were placed in metabolic chambers (TSE Calorimetry Systems, Chesterfield, MO) for 4 d with free access to food and water. During 4 d period, it continuously monitored O_2 consumption, CO_2 production, and ambulatory movement using a photobeam break system. Data were collected every 15 min for 96 h, with the first 36 h considered an acclimatization period and excluded from analyses. Dark-Light cycle was set for 12 h with dark starting at 19.00 h light at 07.00 h. The volume of oxygen consumed (VO_2; [ml/(kg × h)]) and carbon dioxide produced (VCO_2;

[ml/(kg × h)]) were measured to calculate RER (ratio of CO_2 produced to VO_2 consumed)

qRT-PCR from skeletal muscle and Liver to detect gene expression

Skeletal muscle (gastrocnemius) and liver was collected from WT (N = 9) and N2KO (N = 7) 11-14 weeks old mice. Tissues were homogenized into 4 M guanidine isothiocyanate buffer. Samples were layered over 5.7 M cesium chloride buffer and spun for 18 h at 120,000 X *g* at 20^0 C. The supernatant was discarded, and RNA was resuspended in water and stored frozen until use. RNA was then DNAse treated prior to cDNA preparation. cDNA was created using reverse transcriptase in a magnesium buffer (Promega Corp.) for 1 hr at 42^0 C. qRT-PCR was performed using *Power* SYBR® Green, PCR master mix (2X). mRNA levels of each gene of interest was normalized against β–actin. A list of primer sequences used for amplification is found in Table 1. β–actin levels are constant between WT and N2KO animals (9). Normalized levels of mRNA were measured in triplicate per individual mouse from which sample means were calculated for each mouse. Data is presented as the fold-difference relative to the WT control group. For each mRNA amplified, melting-curve analysis was done to confirm the presence of a single amplicon.

Statistical analysis

All values are expressed as mean±SEM unless indicated otherwise. Comparison of means between two groups was made using unpaired two-tailed Student's T-test. Significance is expressed at $p \leq 0.05$ (*); $p \leq 0.01$ (**). Wherever there was more than one variable such as GTT and ITT, statistical analysis was

done by analysis of variance (ANOVA) followed by multicomparison Tukey test. For ANOVA analyses the F value, degrees of freedom (dF) and significance level (*P*-value) are given. Significance was rejected at p≥0.05 (*);

Figure legends

Figure 1: Glucose and insulin tolerance in WT and N2KO mice.

A. Glucose tolerance test on 11 week old mice. WT and N2KO mice were injected with 2mg/kg body weight of D-glucose. Blood glucose levels were measured at 0, 15, 30, 60, 90, 120 and 180 min time points following injection.

B. Insulin Tolerance Test conducted 10 days later using same set of mice as for the glucose tolerance test. Insulin (0.75 units per kg body weight) and blood glucose levels were measured at 0, 15, 30, 60 and 90 min time points. Data are reported as mean blood glucose levels $\pm$ SEM. (*$p \leq 0.05$, **$p \leq 0.01$)

Figure 2: Fatty Acid Oxidation pattern in red, white quadriceps and liver of WT and N2KO animals

Radio-labeled substrates (palmitate) were used to measure FA metabolism in white (**A**), red quadriceps muscle (**B**) and liver (**C**). Fatty Acid Oxidation levels are shown for complete (CO_2) and incomplete (ASMs) as well as total oxidation. Data are presented as mean±SEM. (*$p \leq 0.05$).

Figure 3: Respiratory exchange ratio (RER) of N2KO by using Indirect calorimetry method

RER pattern of N2KO vs WT is shown for 60 h divided into 12 h of dark-light cycle (Figure 3A). Dark and light phase average RER is shown Figure 3B. Data are presented as mean±SEM. (*$p \leq 0.05$).

Figure 4: Skeletal muscle gene expression profile in WT and N2KO mice.

RNA from WT and N2KO whole gastrocnemius muscle was isolated from ad lib fed mice (WT, N=9 and N2KO,N=7) and measured in triplicate using quantitative

RT-PCR for the lipogenic (**A**), Lipolytic (**B**), and PPARs (**C**) gene families. All samples were normalized to β-actin expression. The data is reported as the mean expression level relative to WT expression$\pm$SEM (*$p \leq 0.05$, **$p \leq 0.01$).

Figure 5: Liver gene expression profile in WT and N2KO mice.

RNA from WT and N2KO liver was isolated from ad lib fed mice (WT, N=11 and N2KO, N=9) and the gene expression measured in triplicate using quantitative RT-PCR for the genes involved in lipid metabolism (**A**) and PPARs (**B**) genes. All samples were normalized to β–actin expression. The data is reported as the mean expression level relative to WT expression$\pm$SEM (*$p \leq 0.05$, ** $p \leq 0.01$).

Table 1: Body composition analysis of N2KO mice

Body composition analysis was done on WT (N=9) and N2KO (N=7) (all male age range 10-12 weeks) animals, using the Minispec LF90 (Bruker Optics, Billerica, MA), an NMR analyzer for whole body composition assay of live, unanesthetized mice. Data is reported as a mean±SEM, significance is expressed at (**p<0.01 and ***p<0.001)

	WT (N=9)	**N2KO** (N=7)	**p-value** (**p<0.01 and ***p<0.001)
Body Weight	22.99±1.01	26.43±1.91	0.06
Fat (g)	2.01±0.33	4.64±0.68**	0.002
Fat (%)	8.66±1.24	17.29±1.66***	0.0003
Lean body weight (g)	16.89±0.77	16.81±1.18	0.47

Table 2: Primer sequences used for quantitative real-time RT-PCR assays

All sequences are to the mouse genes, and the forward and reverse primers are indicated.

Gene	Primers	Sequence 5'-- 3'
β-actin	Forward	GGAATCCTGTGGCATCCAT
	Reverse	GGAGGAGCAATGATCTTGATCT
ACC-α	Forward	ATGGGCGGAATGGTCTCTTTC
	Reverse	TGGGGACCTTGTCTTCATCAT
CPT-1α	Forward	AAAGATCAATCGGACCCTAGACA
	Reverse	CAGCGAGTAGCGCATAGTCA
FAS	Forward	AGAGATCCCGAGACGCTTCT
	Reverse	GCCTGGTAGGCATTCTGTAGT
HSL	Forward	CCTCATGGCTCAACTCC
	Reverse	GGTTCTTGACTATGGGTGA
LPL	Forward	AGGACCCCTGAAGACACAG
	Reverse	ACATTCCCGTTACCGTCCATC
PGC-1α	Forward	CGGAAATCATATCCAACCAG
	Reverse	TGAGGACCGCTAGCAAGTTTG
PGC-1β	Forward	AACCCAACCAGTCTCACAGG'
	Reverse	ATGCTGTCCTTGTGGGTAGG
PPAR-α	Forward	TGGGGATGAAGAGGGCTGAG
	Reverse	GGGGACTGCCGTTGTCTGT
PPAR-δ	Forward	ACAGTGACCTGGCGCTCTTC
	Reverse	TGGTGTCCTGGATGGCTTCT
PPAR-γ	Forward	CAGGCTTGCTGAACGTGAAG
	Reverse	GGAGCACCTTGGCGAACA
SCD1	Forward	TGGGTTGGCTGCTTGTG
	Reverse	GCGTGGGCAGGATGAAG
SREBP-1C	Forward	AGCAGCCCCTAGAACAAACAC
	Reverse	CAGCAGTGAGTCTGCCTTGAT

Figure 1

A

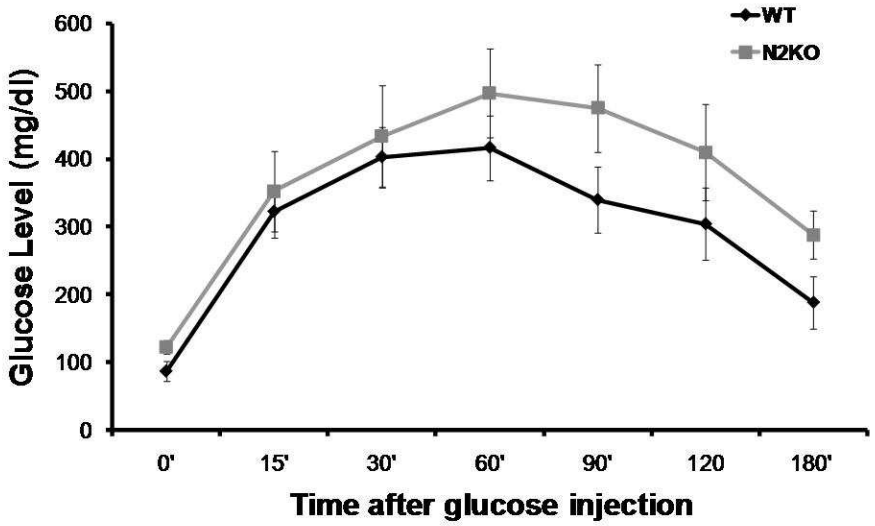
Glucose Tolerance Test
WT
N2KO
Glucose Level (mg/dl)
600
500
400
300
200
100
0
0'
15'
30'
60'
90'
120
180'
Time after glucose injection

B

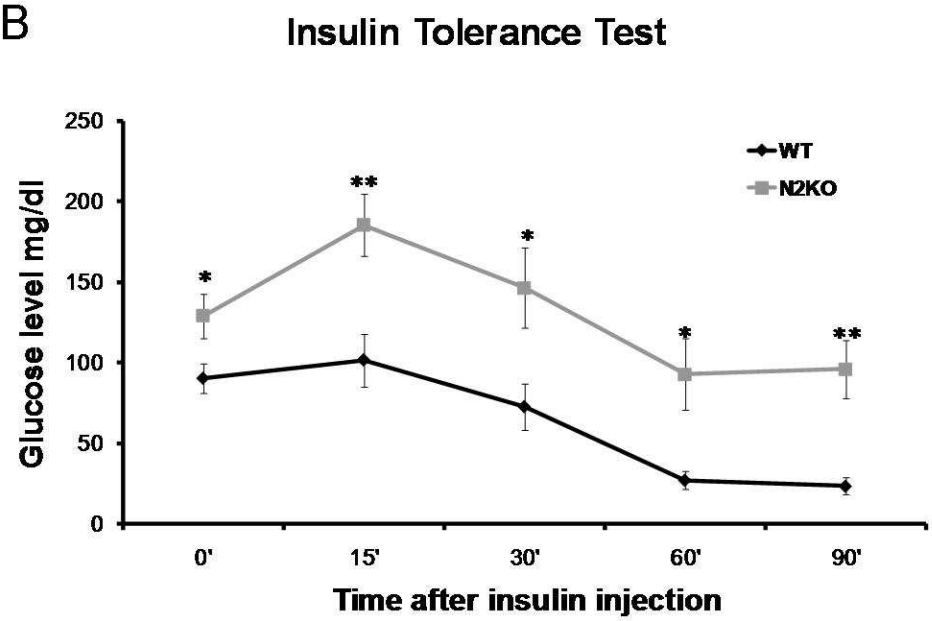
Insulin Tolerance Test
WT
N2KO
Glucose level mg/dl
250
200
150
100
50
0
*
**
*
*
**
0'
15'
30'
60'
90'
Time after insulin injection

Figure 2

A

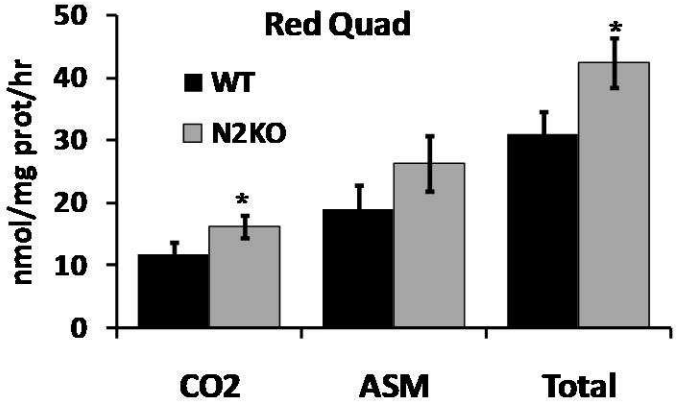
Red Quad
WT
N2KO
nmol/mg prot/hr
50
40
30
20
10
0
*
*
CO2
ASM
Total

B

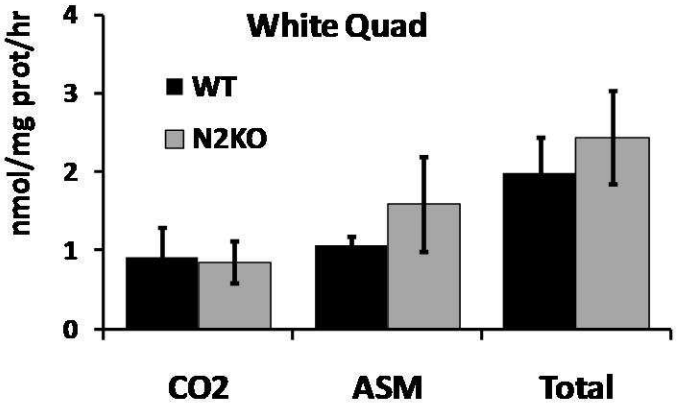
White Quad
WT
N2KO
nmol/mg prot/hr
4
3
2
1
0
CO2
ASM
Total

C

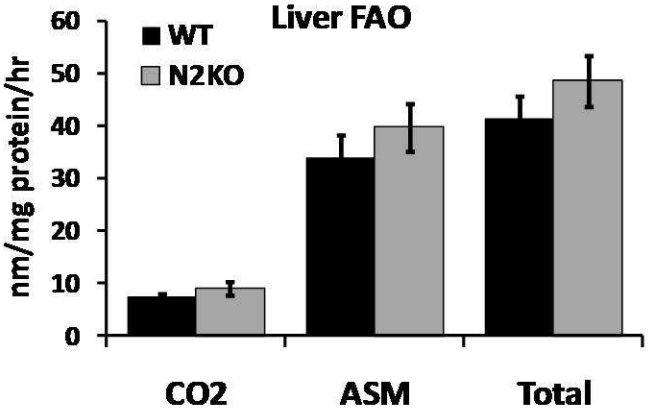
Liver FAO
WT
N2KO
nm/mg protein/hr
60
50
40
30
20
10
0
CO2
ASM
Total

Figure 3

A

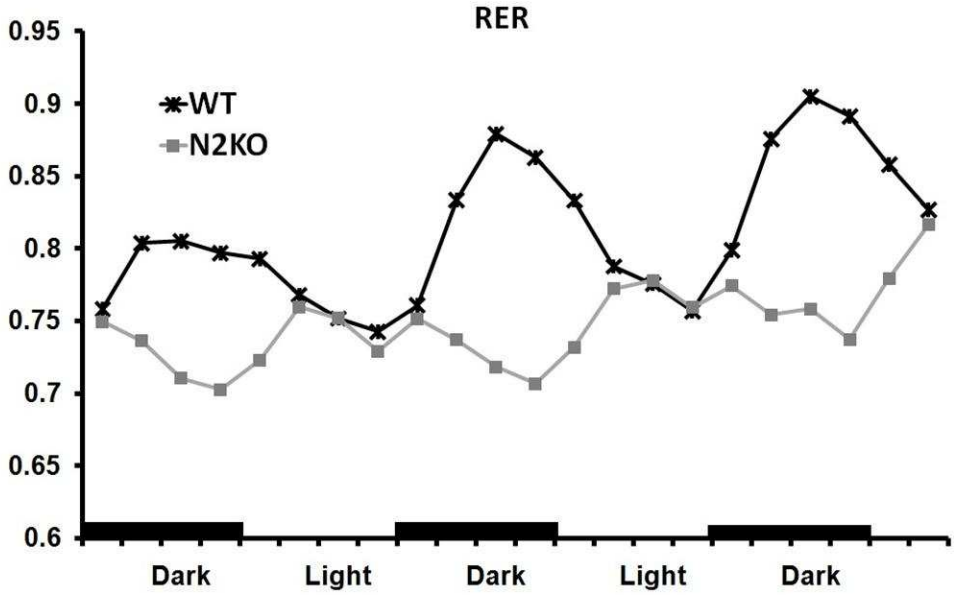
RER
WT
N2KO
0.95
0.9
0.85
0.8
0.75
0.7
0.65
0.6
Dark
Light
Dark
Light
Dark

B

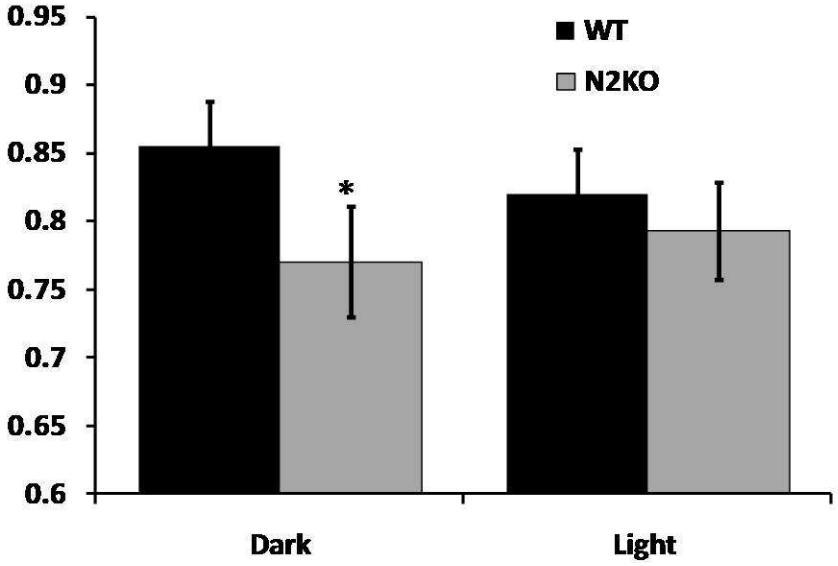
WT
N2KO
0.95
0.9
0.85
0.8
0.75
0.7
0.65
0.6
*
Dark
Light

Figure 4

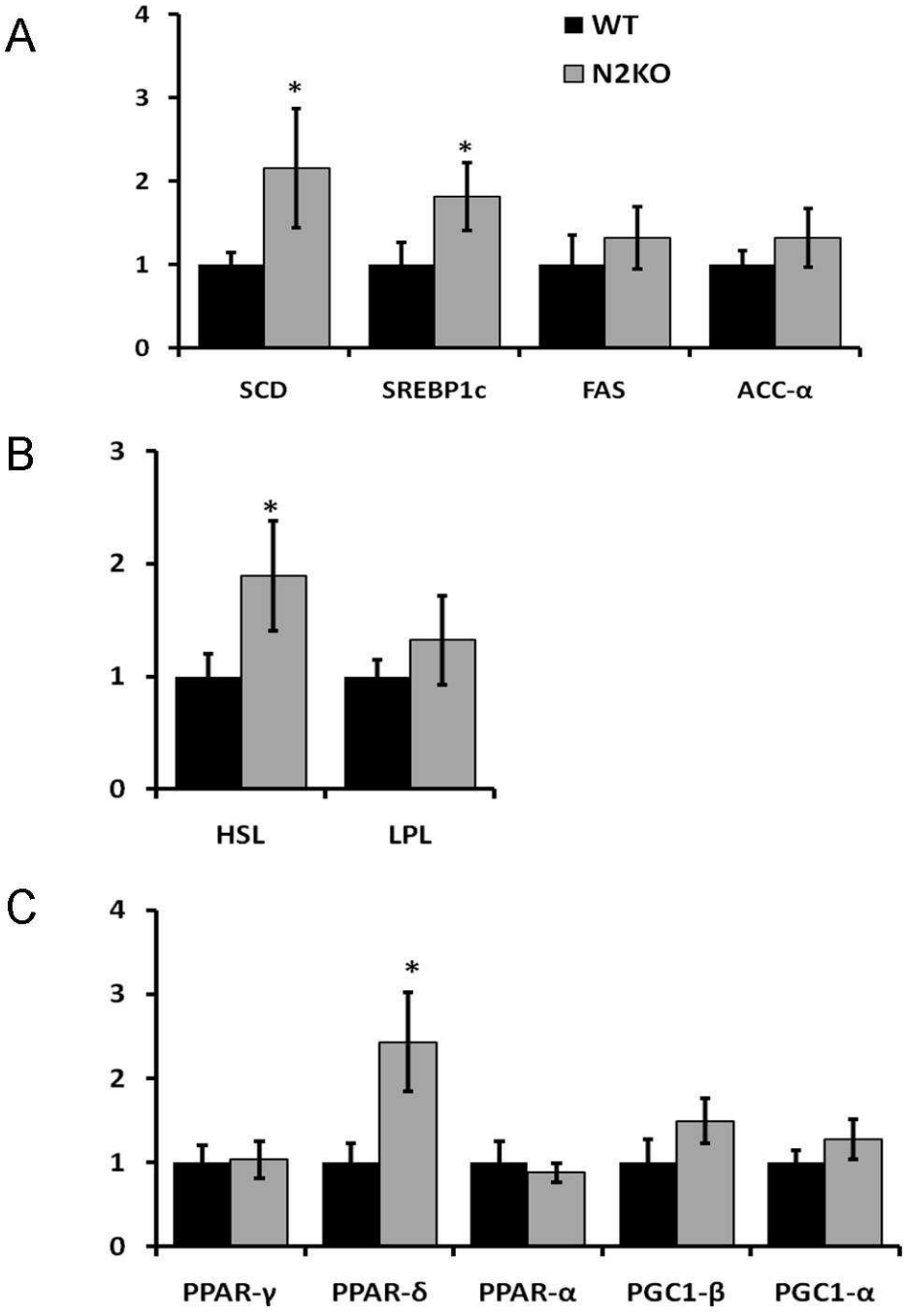
A
WT
N2KO
4
3
2
1
0
*
*
SCD
SREBP1c
FAS
ACC-α
B
3
2
1
0
*
HSL
LPL
C
4
3
2
1
0
*
PPAR-γ
PPAR-δ
PPAR-α
PGC1-β
PGC1-α

Figure 5

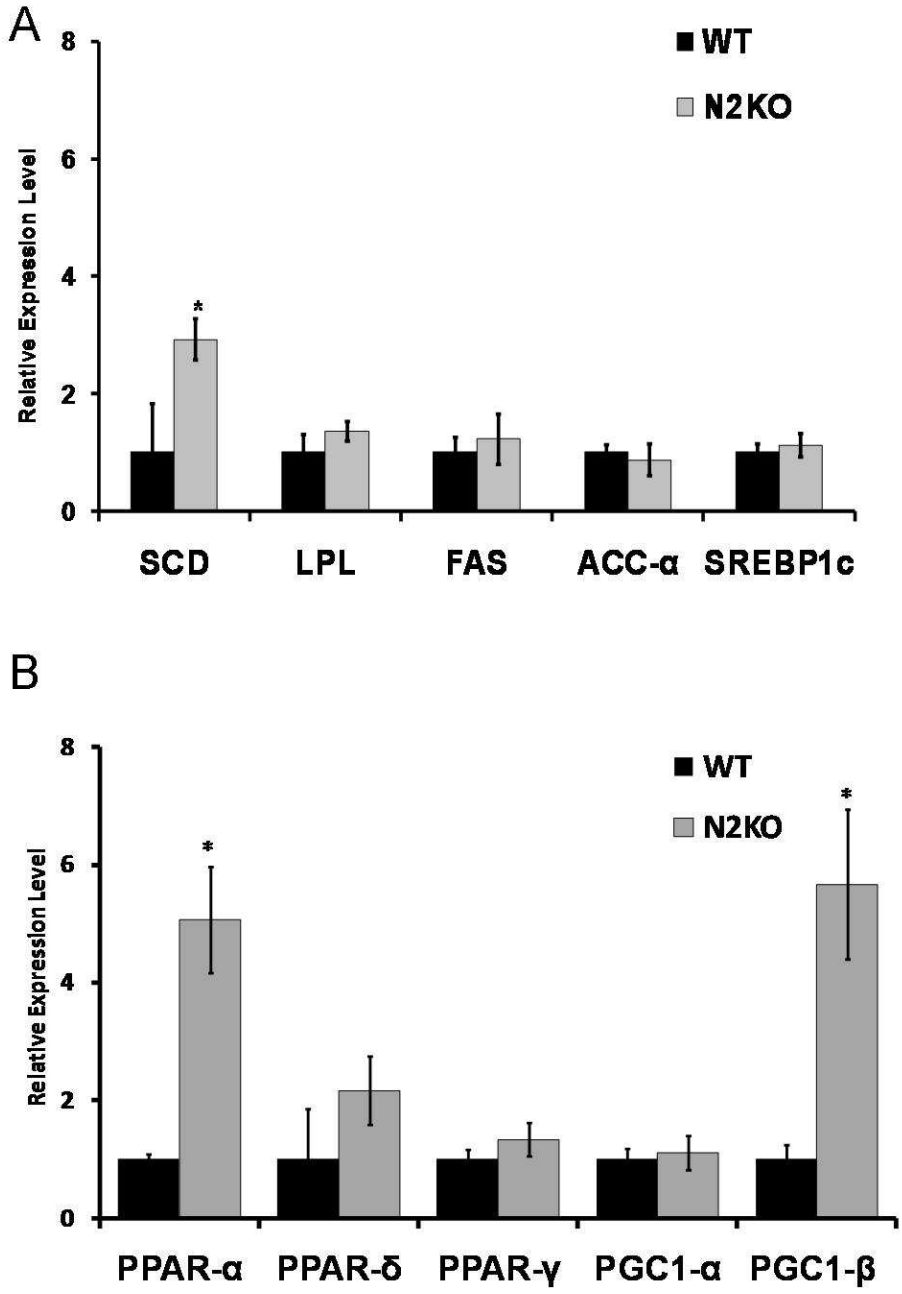
A
WT
N2KO
Relative Expression Level
0
2
4
6
8
*
SCD
LPL
FAS
ACC-α
SREBP1c
B
WT
N2KO
Relative Expression Level
0
2
4
6
8
*
*
PPAR-α
PPAR-δ
PPAR-γ
PGC1-α
PGC1-β

Chapter 6

Implications and future directions

Mutations in the melanocortin pathway, especially those involving the MC4R gene, are one of the most common mutations linked to monogenetic obesity in humans (15). While it is clear that the melanocortin pathway is fundamental to the regulation of body weight, the signaling pathways, transcriptional regulatory mechanisms, its peripheral implications are not well explored. Characterization of these molecular pathways is essential so that therapeutic interventions, behavioral modifications can be done to treat the epidemics of obesity. Experiments performed in this project with the intention of understanding the transcriptional pathways involved in body weight control regulated by Nhlh2 as a transcription factor, have direct relevance to human obesity. Since the genetics has contributed to the cause of obesity immensely it is imminent to study the different mutations/polymorphisms involved in genetic form of obesity. A detailed understanding of the regulatory mechanism of the genes involved in body weight maintenance is critical to understand the basic physiology of the body weight maintenance. Nhlh2 is one of the transcription factor which has already been reported to play an important role in regulating the genes involved in such mechanism, provides an excellent tool to study the underpinnings of body weight maintenance.

N2KO is the only model with targeted deletion of neuronal bHLH transcription factor leading to adult onset obesity. Research so far has shown that Nhlh2 plays an important role in different physiological functions mainly

being body weight maintenance. Here in this project we tried to establish Nhlh2 as a transcriptional regulator of melanocortin 4 receptor. During this project, we asked key questions about the transcriptional regulation of Mc4r and downstream peripheral effects of lowered melanocortin signaling. We are able to show that Nhlh2 regulates Mc4r transcription by binding to the three E-Boxes sites located on Mc4r promoter, and that consistent with lowered melanocortin tone, there was aberrant energy and glucose metabolism in peripheral tissues of the mutant animals. Findings from the present project will help to link human genetic mutations to changes in transcriptional regulation by Nhlh2, and ultimately the phenotypes of overweight and obese in the human population.

During the first part of the project we showed that Nhlh2 binds to three E-Boxes located on Mc4r promoter and regulate the transcription. Mutation in one of those three E-Box ($MC4R^{\Delta GC}$) has already been shown responsible for human obesity (4). The second of these three E-Box mutations is found in both obese and non-obese controls at a frequency of 5%. This mutation -178 A/C, changes E-Box #1 from CATCTG to AATCTG (36). These polymorphisms affect the binding sites of Nhlh2. With the help of *in vitro* studies performed in this project we were able to understand the actual mechanism might be happening in obese individual with these mutations.

In the second part of the project, by using N2KO mice, we studied the tissue specific effects of targeted deletion of Nhlh2. N2KO mice have impairment in glucose and insulin homeostasis. Energy expenditure and fatty acid oxidation pattern is altered and gene expression also varies compared to WT. Adipose

tissue both brown and white has a tissue specific effects because of deletion of Nhlh2. BAT and WAT both has reduced sympathetic innervation and WAT shows the state of inflammation. Results from this experiment gave us an understanding of how events might be unfolding in the obese humans having obesity with Mc4r mutations. This was first attempt to fully characterize the N2KO mouse's metabolism. Findings from this experiment will help us to understand the actual turn of events in humans and will aid us to devise better therapeutic regimen or behavioral modifications.

Possible mechanism for adult onset obesity and transcriptional regulation of Mc4r can be explained in Figure 1. Nhlh2's energy dependent expression and its role as a transcriptional regulator of PC1/3 is already been reported by our laboratory (9, 23). Results of this project establish Nhlh2 as a direct transcriptional regulator of another key body weight regulatory gene, Mc4r. The new work presented in this dissertation firmly situates Nhlh2 as a key transcriptional regulator of the melanocortin pathway.

Taken together, results presented here in establish the Nhlh2's role as a transcriptional regulator of Mc4r and a key part of the melanocortin signaling pathway. Characterization of metabolic phenotype revealed many of the interesting facets of N2KO mouse model which can now be used to help us understand the adult onset obesity at molecular level, and also to further design study that could provide clinical measures to prevent human obesity.

Future Directions

Results from the present project have given a better insight into monogenic form of obesity. It will help to understand a molecular and physiological aspect of obesity of genetic origin. In future, there are several directions which will help us better our understandings towards monogenetic form of obesity.

First of all, as explained in Figure 1, reduced melanocortinergic tone is one of the possibilities stated in N2KO mouse model for developing the peripheral defects. Future experiment should include restoration of melanocortinergic tone and determination of whether melanocortinergic agonists such as melanotan II could restore the normal phenotype in N2KO. N2KO's metabolic phenotype needs to be further explored in detail with respect to indirect calorimetry and glucose homeostasis measurements. These studies include the use of hypyerinsulinemic euglycemic clamps to unravel the actual insulin/glucose homeostasis in N2KOs.

Another direction would be to explore more gene targets involved in same neurocircuitry as Mc4r and PC1/3 is involved i.e. melanocortin pathway. Previous studies have shown that Nhlh2 has the potential to influence the transcription of 1000s of genes (111) and there is a possibility that there are more genes in melanocortin pathway which may be regulated by Nhlh2. These types of experiments will help to put the pieces together which we are missing in the present project.

Inflammatory state of WAT and increased expression of IL-6 in N2KO has opened another interesting area for further exploration. Significant increase in IL-6 expression at mRNA level and serum level makes one wonder if Nhlh2 and IL-6 share some connection. Age wise expression analysis of IL-6 will give better idea that whether state of inflammation is moreover a cause and effect relationship or Nhlh2 has an innate role in IL-6 regulation.

Point mutations in other members of the melanocortin pathway, including MC4R POMC and PC1/3 lead to monogenetic forms of human obesity. There are also point mutations in NHLH2 which are linked to human obesity. In a moderately sized study of 379 obese and 379 lean individuals, a nonsynonymous mutation in human NHLH2 was found in 2 obese and 1 lean individuals(112). Subsequent to that analysis, one of the authors reported that this mutation was only found in obese individuals (113), and that the frequency of the mutation was 0.001 (0.1 percent) in obese individuals (113). While the SNP has not yet been entered into the SNP database (NCBI), the subsequent study identified the position as nucleotide 255 in exon 3, within the coding region of NHLH2. In studies outside of the scope of this proposal, we designed a mutagenized mouse protein to mimic a human mutation in NHLH2 which results in an arginine to proline mutation in the protein. Transfection of this construct into hypothalamic cells showed that the mutant protein product had a reduced size compared to the WT protein (Wankhade, Bush and Good, unpublished).

In another set of studies, Dr. Good found polymorphisms in the 3'-tail of NHLH2 which disrupts a putative miRNA-binding site. In a collaboration with Dr.

Donald Bowden's group at Wake Forest University, 509 African Americans from the Insulin Resistance Atherosclerosis Family Study (114) were screened and found a significant association with BMI adjusted waist measurements ($p = 0.043$) and waist-hip ratios ($p = 0.035$) for this newly found polymorphism rs11805084 ($NHLH2^{A1568G}$). Thus, while rare in the human population, mutations in NHLH2 exist and appear to contribute to differences in human body weight regulation. More studies are needed on NHLH2 in human populations to further characterize its role in the genetic basis of obesity in populations.

By using the knowledge gained from studies of this type, many questions and future directions are now ready to be answered. The N2KO mouse model is one that can be used to answer molecular and whole-body physiological questions about the role of each of the members of melanocortin signaling pathway in body weight regulation.

Figure 1: Hypothetical model of Nhlh2 regulation of melanocortin cascades in brain and its peripheral effects

Nhlh2 regulates PC1/3 gene transcription and acts on POMC neuron which is also stimulated by serum leptin level through leptin receptor and controls α-MSH, endogenous ligand of MC4R. Results from the present project states that Nhlh2 acts as transcriptional regulator of Mc4r. Reduced melanocortinergic tone in N2KO may exhibits its tissue specific effects of adult onset obesity.

Figure 1

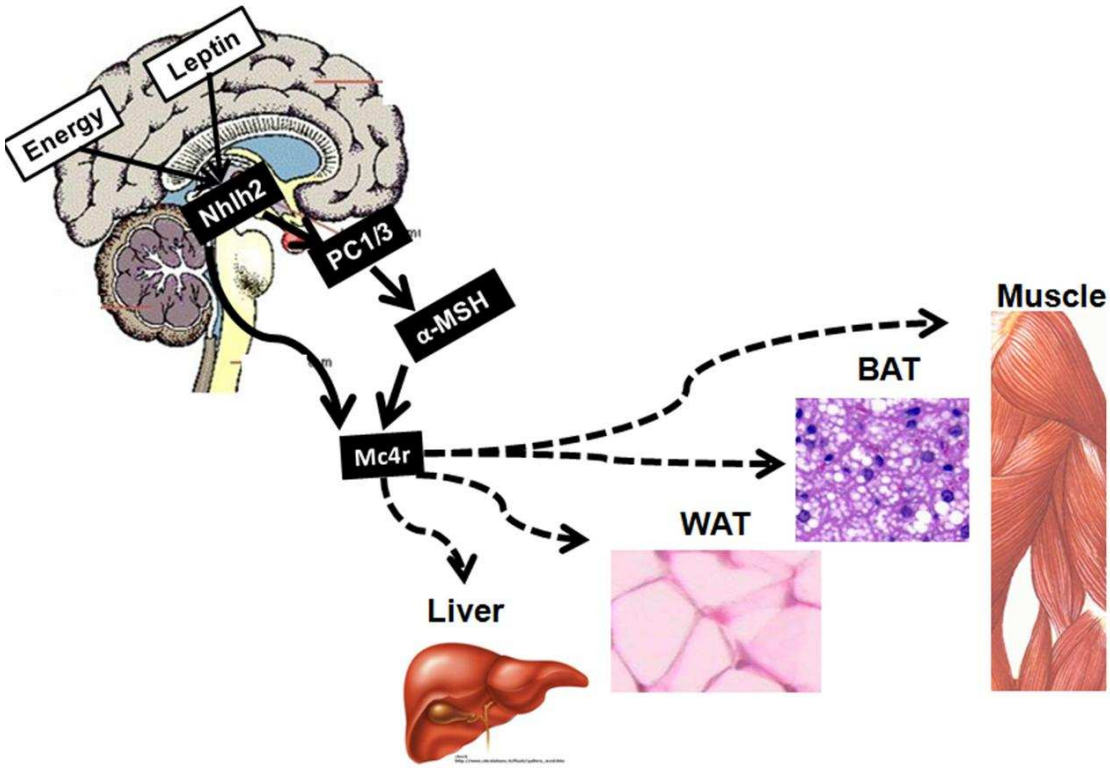

Appendix

Figure 1: Effects of double and triple mutants on Mc4r transactivation in presence of Nhlh2.

A. Substitution mutations in all three E-Box sites in combination were created by site directed mutagenesis. Mc4r-Mut-1/2 has mutation in 1st and 2nd E-Box, Mc4r-Mut-1/3 has mutation in 1st and 3rd E-Box, Mc4r-Mut-2/3 has a mutation in 2nd and 3rd E-Box and Mc4r-Mut-1/2/3 plasmid has Mc4r promoter with all three sites mutated.

B. Transactivation assays performed by using WT Mc4r promoter and with the promoter with mutations in each individual E-Box motifs. Activity of the WT Mc4r-luc reporter (WT) transfected into N29/2 cells in the presence (*black bars*) or absence (*gray bars*) of Nhlh2. The luciferase activity was measured and normalized to the expression of β-gal-encoding protein. Activity is presented relative to the values obtained in cells transfected with PGL3-luc alone ± SE. **, $p < 0.01$; to empty vector expression.

Figure 2: Fatty Acid Oxidation pattern in red, white quadriceps and gene expression in gastrocnemius muscle of WT and N2KO animals (12 hr Food deprived)

A. Radio-labeled substrates (palmitate) were used to measure FA metabolism in white, red quadriceps muscle and liver. Fatty Acid Oxidation levels are shown for complete (CO_2) and incomplete (ASMs) as well as total oxidation. Data are presented as mean±SEM. (*$p \leq 0.05$).

B. Skeletal muscle gene expression profile in WT and N2KO mice.

RNA from WT and N2KO whole gastrocnemius muscle was isolated from ad lib fed mice (WT N=8 and N2KO=6) and measured in triplicate using quantitative RT-PCR. All samples were normalized to β-actin expression. The data is reported as the mean expression level relative to WT expression$\pm$SEM (*$p \leq 0.05$, **$p \leq 0.01$).

Figure 1

A.

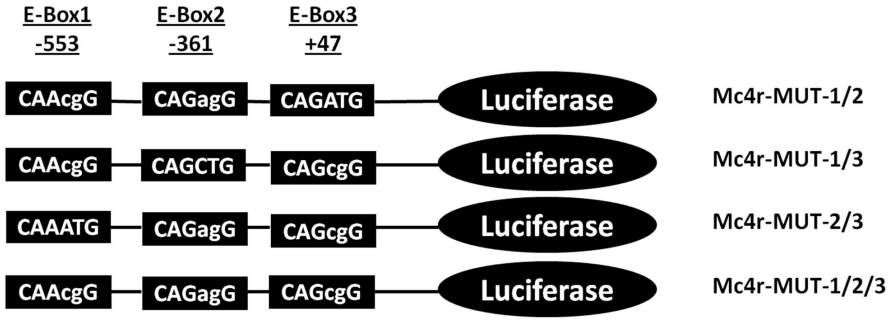
E-Box1
-553
E-Box2
-361
E-Box3
+47
CAAcgG
CAGagG
CAGATG
Luciferase
Mc4r-MUT-1/2
CAAcgG
CAGCTG
CAGcgG
Luciferase
Mc4r-MUT-1/3
CAAATG
CAGagG
CAGcgG
Luciferase
Mc4r-MUT-2/3
CAAcgG
CAGagG
CAGcgG
Luciferase
Mc4r-MUT-1/2/3

B.

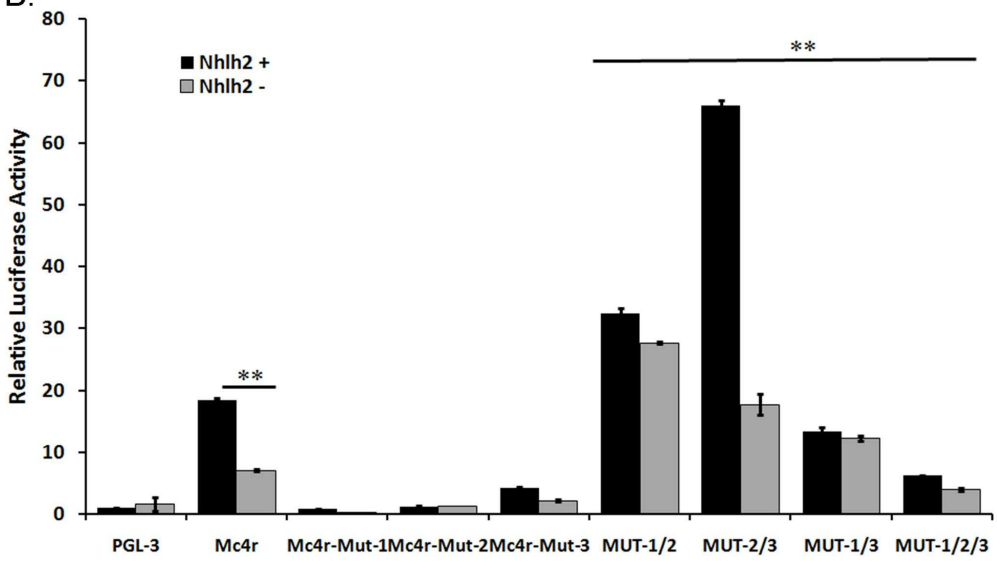
Nhlh2 +
Nhlh2 -
Relative Luciferase Activity
80
70
60
50
40
30
20
10
0
**
**
PGL-3
Mc4r
Mc4r-Mut-1
Mc4r-Mut-2
Mc4r-Mut-3
MUT-1/2
MUT-2/3
MUT-1/3
MUT-1/2/3

Figure 2

A

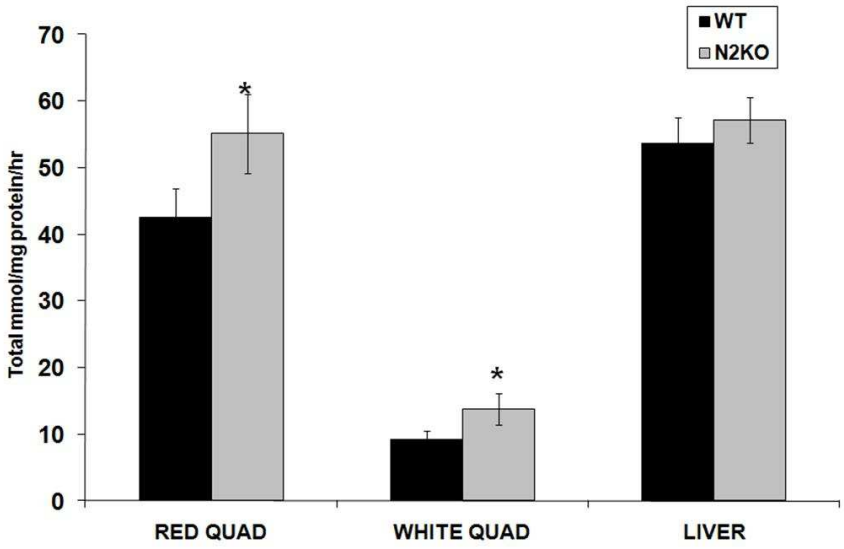
WT
N2KO
Total mmol/mg protein/hr
70
60
50
40
30
20
10
0
*
*
RED QUAD
WHITE QUAD
LIVER

B

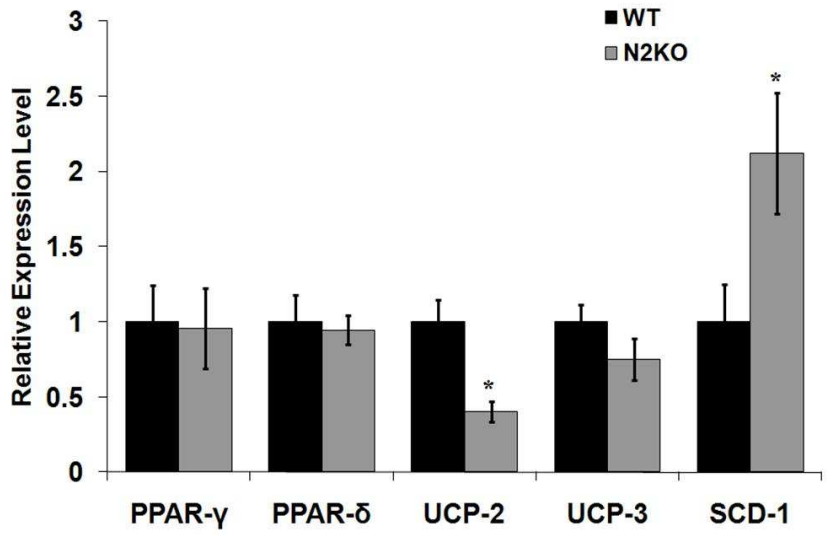
WT
N2KO
Relative Expression Level
3
2.5
2
1.5
1
0.5
0
*
*
PPAR-γ
PPAR-δ
UCP-2
UCP-3
SCD-1

References

1. CDC 2006 BMI- Body Mass Index: BMI for Adults: . CDC 2007:1
2. Flegal KM, Carroll MD, Ogden CL, Curtin LR 2010 Prevalence and trends in obesity among US adults, 1999-2008. JAMA 303:235-241
3. Finkelstein EA, Fiebelkorn IC, Wang G 2003 National medical spending attributable to overweight and obesity: how much, and who's paying? Health Aff (Millwood) Suppl Web Exclusives:W3-219-226
4. Valli-Jaakola K, Palvimo JJ, Lipsanen-Nyman M, Salomaa V, Peltonen L, Kontula K, Schalin-Jantti C 2006 A two-base deletion -439delGC in the melanocortin-4 receptor promoter associated with early-onset obesity. Horm Res 66:61-69
5. Loos RJ, Rankinen T, Tremblay A, Perusse L, Chagnon Y, Bouchard C 2004 Melanocortin-4 receptor gene and physical activity in the Quebec Family Study. Int J Obes Relat Metab Disord
6. Allan DW, Thor S 2003 Together at last: bHLH and LIM-HD regulators cooperate to specify motor neurons. Neuron 38:675-677
7. Atchley WR, Fitch WM 1997 A natural classification of the basic helix-loop-helix class of transcription factors. Proc Natl Acad Sci U S A 94:5172-5176
8. Blanar MA, Rutter WJ 1992 Interaction cloning: identification of a helix-loop-helix zipper protein that interacts with c-Fos. Science 256:1014-1018

9. Vella KR, Burnside AS, Brennan KM, Good DJ 2007 Expression of the hypothalamic transcription factor Nhlh2 is dependent on energy availability. J Neuroendocrinol 19:499-510

10. Jing E, Nillni EA, Sanchez VC, Stuart RC, Good DJ 2004 Deletion of the Nhlh2 transcription factor decreases the levels of the anorexigenic peptides alpha melanocyte-stimulating hormone and thyrotropin-releasing hormone and implicates prohormone convertases I and II in obesity. Endocrinology 145:1503-1513

11. Good DJ, Porter FD, Mahon KA, Parlow AF, Westphal H, Kirsch IR 1997 Hypogonadism and obesity in mice with a targeted deletion of the Nhlh2 gene. Nat Genet 15:397-401

12. Coyle CA, Jing E, Hosmer T, Powers JB, Wade G, Good DJ 2002 Reduced voluntary activity precedes adult-onset obesity in Nhlh2 knockout mice. Physiol Behav 77:387-402

13. Balthasar N 2006 Genetic dissection of neuronal pathways controlling energy homeostasis. Obesity (Silver Spring) 14 Suppl 5:222S-227S

14. Bates SH, Dundon TA, Seifert M, Carlson M, Maratos-Flier E, Myers MG, Jr. 2004 LRb-STAT3 signaling is required for the neuroendocrine regulation of energy expenditure by leptin. Diabetes 53:3067-3073

15. Farooqi S, O'Rahilly S 2006 Genetics of obesity in humans. Endocr Rev 27:710-718

16. Cai G, Cole SA, Butte N, Bacino C, Diego V, Tan K, Goring HH, O'Rahilly S, Farooqi IS, Comuzzie AG 2006 A quantitative trait locus on

chromosome 18q for physical activity and dietary intake in Hispanic children. Obesity (Silver Spring) 14:1596-1604

17. Ste Marie L, Miura GI, Marsh DJ, Yagaloff K, Palmiter RD 2000 A metabolic defect promotes obesity in mice lacking melanocortin-4 receptors. Proc Natl Acad Sci U S A 97:12339-12344

18. Nogueiras R, Wiedmer P, Perez-Tilve D, Veyrat-Durebex C, Keogh JM, Sutton GM, Pfluger PT, Castaneda TR, Neschen S, Hofmann SM, Howles PN, Morgan DA, Benoit SC, Szanto I, Schrott B, Schurmann A, Joost HG, Hammond C, Hui DY, Woods SC, Rahmouni K, Butler AA, Farooqi IS, O'Rahilly S, Rohner-Jeanrenaud F, Tschop MH 2007 The central melanocortin system directly controls peripheral lipid metabolism. J Clin Invest 117:3475-3488

19. Butler AA, Marks DL, Fan W, Kuhn CM, Bartolome M, Cone RD 2001 Melanocortin-4 receptor is required for acute homeostatic responses to increased dietary fat. Nat Neurosci 4:605-611

20. Bartness TJ, Kay Song C, Shi H, Bowers RR, Foster MT 2005 Brain-adipose tissue cross talk. Proc Nutr Soc 64:53-64

21. Foster MT, Bartness TJ 2006 Sympathetic but not sensory denervation stimulates white adipocyte proliferation. Am J Physiol Regul Integr Comp Physiol 291:R1630-1637

22. Obici S, Feng Z, Tan J, Liu L, Karkanias G, Rossetti L 2001 Central melanocortin receptors regulate insulin action. J Clin Invest 108:1079-1085

23. Fox DL, Good DJ 2008 Nescient helix-loop-helix 2 interacts with signal transducer and activator of transcription 3 to regulate transcription of prohormone convertase 1/3. Mol Endocrinol 22:1438-1448

24. Allison DB, Heshka S, Neale MC, Lykken DT, Heymsfield SB 1994 A genetic analysis of relative weight among 4,020 twin pairs, with an emphasis on sex effects. Health Psychol 13:362-365

25. Comuzzie AG, Blangero J, Mahaney MC, Mitchell BD, Hixson JE, Samollow PB, Stern MP, MacCluer JW 1995 Major gene with sex-specific effects influences fat mass in Mexican Americans. Genet Epidemiol 12:475-488

26. Comuzzie AG, Blangero J, Mahaney MC, Haffner SM, Mitchell BD, Stern MP, MacCluer JW 1996 Genetic and environmental correlations among hormone levels and measures of body fat accumulation and topography. J Clin Endocrinol Metab 81:597-600

27. Kopelman PG 2000 Obesity as a medical problem. Nature 404:635-643

28. Prochazka M, Leiter EH 1991 Effect of androgen insensitivity on diabetogenesis in db/db male mice with testicular feminization (Tfm). Horm Metab Res 23:149-154

29. Hall C, Manser E, Spurr NK, Lim L 1993 Assignment of the human carboxypeptidase E (CPE) gene to chromosome 4. Genomics 15:461-463

30. Geffroy S, De Vos P, Staels B, Duban B, Auwerx J, de Martinville B 1995 Localization of the human OB gene (OBS) to chromosome 7q32 by fluorescence in situ hybridization. Genomics 28:603-604

31. Tartaglia LA, Dembski M, Weng X, Deng N, Culpepper J, Devos R, Richards GJ, Campfield LA, Clark FT, Deeds J, Muir C, Sanker S, Moriarty A, Moore KJ, Smutko JS, Mays GG, Wool EA, Monroe CA, Tepper RI 1995 Identification and expression cloning of a leptin receptor, OB-R. Cell 83:1263-1271

32. Kleyn PW, Fan W, Kovats SG, Lee JJ, Pulido JC, Wu Y, Berkemeier LR, Misumi DJ, Holmgren L, Charlat O, Woolf EA, Tayber O, Brody T, Shu P, Hawkins F, Kennedy B, Baldini L, Ebeling C, Alperin GD, Deeds J, Lakey ND, Culpepper J, Chen H, Glucksmann-Kuis MA, Carlson GA, Duyk GM, Moore KJ 1996 Identification and characterization of the mouse obesity gene tubby: a member of a novel gene family. Cell 85:281-290

33. Huszar D, Lynch CA, Fairchild-Huntress V, Dunmore JH, Fang Q, Berkemeier LR, Gu W, Kesterson RA, Boston BA, Cone RD, Smith FJ, Campfield LA, Burn P, Lee F 1997 Targeted disruption of the melanocortin-4 receptor results in obesity in mice. Cell 88:131-141

34. Mountjoy KG, Wong J 1997 Obesity, diabetes and functions for proopiomelanocortin-derived peptides. Mol Cell Endocrinol 128:171-177

35. Vella KR, Good DJ 2010 Nhlh2 is a Cold-Responsive Gene. The Open Neuroendocrinology Journal 3:38-44

36. Lubrano-Berthelier C, Cavazos M, Le Stunff C, Haas K, Shapiro A, Zhang S, Bougneres P, Vaisse C 2003 The Human MC4R Promoter: Characterization and Role in Obesity. Diabetes 52:2996-3000

37. Daniel PB, Fernando C, Wu CS, Marnane R, Broadhurst R, Mountjoy KG 2005 1 kb of 5' flanking sequence from mouse MC4R gene is sufficient for tissue specific expression in a transgenic mouse. Mol Cell Endocrinol 239:63-71

38. Staubert C, Tarnow P, Brumm H, Pitra C, Gudermann T, Gruters A, Schoneberg T, Biebermann H, Rompler H 2007 Evolutionary Aspects in Evaluating Mutations in the Melanocortin 4 Receptor. Endocrinology 148:4642-4648

39. Belsham DD, Cai F, Cui H, Smukler SR, Salapatek AM, Shkreta L 2004 Generation of a phenotypic array of hypothalamic neuronal cell models to study complex neuroendocrine disorders. Endocrinology 145:393-400

40. Kruger M, Ruschke K, Braun T 2004 NSCL-1 and NSCL-2 synergistically determine the fate of GnRH-1 neurons and control necdin gene expression. Embo J 23:4353-4364

41. Johnson SA, Marin-Bivens CL, Miele M, Coyle CA, Fissore R, Good DJ 2004 The Nhlh2 transcription factor is required for female sexual behavior and reproductive longevity. Horm Behav 46:420-427

42. Han C, Liu H, Liu J, Yin K, Xie Y, Shen X, Wang Y, Yuan J, Qiang B, Liu YJ, Peng X 2005 Human Bex2 interacts with LMO2 and regulates the transcriptional activity of a novel DNA-binding complex. Nucleic Acids Res 33:6555-6565

43. Zhang Y, Proenca R, Maffei M, Barone M, Leopold L, Friedman JM 1994 Positional cloning of the mouse obese gene and its human homologue. Nature 372:425-432

44. Flier JS 2004 Obesity wars: molecular progress confronts an expanding epidemic. Cell 116:337-350

45. Nedergaard J, Bengtsson T, Cannon B 2007 Unexpected evidence for active brown adipose tissue in adult humans. Am J Physiol Endocrinol Metab 293:E444-452

46. Cypess AM, Lehman S, Williams G, Tal I, Rodman D, Goldfine AB, Kuo FC, Palmer EL, Tseng YH, Doria A, Kolodny GM, Kahn CR 2009 Identification and importance of brown adipose tissue in adult humans. N Engl J Med 360:1509-1517

47. Saito M, Okamatsu-Ogura Y, Matsushita M, Watanabe K, Yoneshiro T, Nio-Kobayashi J, Iwanaga T, Miyagawa M, Kameya T, Nakada K, Kawai Y, Tsujisaki M 2009 High incidence of metabolically active brown adipose tissue in healthy adult humans: effects of cold exposure and adiposity. Diabetes 58:1526-1531

48. Bartness TJ, Bamshad M 1998 Innervation of mammalian white adipose tissue: implications for the regulation of total body fat. Am J Physiol 275:R1399-1411

49. Brodie BB, Costa E, Dlabac A, Neff NH, Smookler HH 1966 Application of steady state kinetics to the estimation of synthesis rate and turnover time of tissue catecholamines. J Pharmacol Exp Ther 154:493-498

50. Dodt C, Lonnroth P, Wellhoner JP, Fehm HL, Elam M 2003 Sympathetic control of white adipose tissue in lean and obese humans. Acta Physiol Scand 177:351-357

51. Youngstrom TG, Bartness TJ 1995 Catecholaminergic innervation of white adipose tissue in Siberian hamsters. Am J Physiol 268:R744-751

52. Garofalo MA, Kettelhut IC, Roselino JE, Migliorini RH 1996 Effect of acute cold exposure on norepinephrine turnover rates in rat white adipose tissue. J Auton Nerv Syst 60:206-208

53. Migliorini RH, Garofalo MA, Kettelhut IC 1997 Increased sympathetic activity in rat white adipose tissue during prolonged fasting. Am J Physiol 272:R656-661

54. Moinat M, Deng C, Muzzin P, Assimacopoulos-Jeannet F, Seydoux J, Dulloo AG, Giacobino JP 1995 Modulation of obese gene expression in rat brown and white adipose tissues. FEBS Lett 373:131-134

55. Hardie LJ, Rayner DV, Holmes S, Trayhurn P 1996 Circulating leptin levels are modulated by fasting, cold exposure and insulin administration in lean but not Zucker (fa/fa) rats as measured by ELISA. Biochem Biophys Res Commun 223:660-665

56. Trayhurn P, Thomas ME, Duncan JS, Rayner DV 1995 Effects of fasting and refeeding on ob gene expression in white adipose tissue of lean and obese (oblob) mice. FEBS Lett 368:488-490

57. Foster MT, Song CK, Bartness TJ 2009 Hypothalamic Paraventricular Nucleus Lesion Involvement in the Sympathetic Control of Lipid Mobilization. Obesity (Silver Spring)

58. Cantu RC, Goodman HM 1967 Effects of denervation and fasting on white adipose tissue. Am J Physiol 212:207-212

59. Bray GA, Nishizawa Y 1978 Ventromedial hypothalamus modulates fat mobilisation during fasting. Nature 274:900-902

60. Song CK, Vaughan CH, Keen-Rhinehart E, Harris RB, Richard D, Bartness TJ 2008 Melanocortin-4 receptor mRNA expressed in sympathetic outflow neurons to brown adipose tissue: neuroanatomical and functional evidence. Am J Physiol Regul Integr Comp Physiol 295:R417-428

61. Brito MN, Brito NA, Baro DJ, Song CK, Bartness TJ 2007 Differential activation of the sympathetic innervation of adipose tissues by melanocortin receptor stimulation. Endocrinology 148:5339-5347

62. Bartness TJ, Song CK 2007 Brain-adipose tissue neural crosstalk. Physiol Behav 91:343-351

63. Collins S, Cao W, Robidoux J 2004 Learning new tricks from old dogs: beta-adrenergic receptors teach new lessons on firing up adipose tissue metabolism. Mol Endocrinol 18:2123-2131

64. Nagase I, Yoshida T, Kumamoto K, Umekawa T, Sakane N, Nikami H, Kawada T, Saito M 1996 Expression of uncoupling protein in skeletal

muscle and white fat of obese mice treated with thermogenic beta 3-adrenergic agonist. J Clin Invest 97:2898-2904

65. 2010 In; Allen Institute for Brain Science

66. Good DJ, Coyle CA, Fox DL 2008 Nhlh2: a basic helix-loop-helix transcription factor controlling physical activity. Exerc Sport Sci Rev 36:187-192

67. Flier JS 1998 Clinical review 94: What's in a name? In search of leptin's physiologic role. J Clin Endocrinol Metab 83:1407-1413

68. Swoap SJ, Weinshenker D 2008 Norepinephrine controls both torpor initiation and emergence via distinct mechanisms in the mouse. PLoS One 3:e4038

69. Rikke BA, Yerg JE, 3rd, Battaglia ME, Nagy TR, Allison DB, Johnson TE 2003 Strain variation in the response of body temperature to dietary restriction. Mech Ageing Dev 124:663-678

70. Youngstrom TG, Bartness TJ 1998 White adipose tissue sympathetic nervous system denervation increases fat pad mass and fat cell number. Am J Physiol 275:R1488-1493

71. Ruschke K, Ebelt H, Kloting N, Boettger T, Raum K, Bluher M, Braun T 2009 Defective peripheral nerve development is linked to abnormal architecture and metabolic activity of adipose tissue in Nscl-2 mutant mice. PLoS One 4:e5516

72. Swoap SJ, Gutilla MJ, Liles LC, Smith RO, Weinshenker D 2006 The full expression of fasting-induced torpor requires beta 3-adrenergic receptor signaling. J Neurosci 26:241-245

73. Lazzarini SJ, Wade GN 1991 Role of sympathetic nerves in effects of estradiol on rat white adipose tissue. Am J Physiol 260:R47-51

74. Good DJ 2007 Obese Mouse Models. In: Conn PM ed. Sourcebook of Models for Biomedical Research. Totowa, New Jersey: Humana; 683-702

75. Bamshad M, Aoki VT, Adkison MG, Warren WS, Bartness TJ 1998 Central nervous system origins of the sympathetic nervous system outflow to white adipose tissue. Am J Physiol 275:R291-299

76. Bamshad M, Song CK, Bartness TJ 1999 CNS origins of the sympathetic nervous system outflow to brown adipose tissue. Am J Physiol 276:R1569-1578

77. Gettys TW, Harkness PJ, Watson PM 1996 The beta 3-adrenergic receptor inhibits insulin-stimulated leptin secretion from isolated rat adipocytes. Endocrinology 137:4054-4057

78. Muzzin P, Revelli JP, Kuhne F, Gocayne JD, McCombie WR, Venter JC, Giacobino JP, Fraser CM 1991 An adipose tissue-specific beta-adrenergic receptor. Molecular cloning and down-regulation in obesity. J Biol Chem 266:24053-24058

79. Emorine LJ, Marullo S, Briend-Sutren MM, Patey G, Tate K, Delavier-Klutchko C, Strosberg AD 1989 Molecular characterization of the human beta 3-adrenergic receptor. Science 245:1118-1121

80. Nahmias C, Blin N, Elalouf JM, Mattei MG, Strosberg AD, Emorine LJ 1991 Molecular characterization of the mouse beta 3-adrenergic receptor: relationship with the atypical receptor of adipocytes. EMBO J 10:3721-3727

81. Granneman JG, Lahners KN, Chaudhry A 1991 Molecular cloning and expression of the rat beta 3-adrenergic receptor. Mol Pharmacol 40:895-899

82. Granneman JG, Lahners KN, Chaudhry A 1993 Characterization of the human beta 3-adrenergic receptor gene. Mol Pharmacol 44:264-270

83. Nonogaki K, Strack AM, Dallman MF, Tecott LH 1998 Leptin-independent hyperphagia and type 2 diabetes in mice with a mutated serotonin 5-HT2C receptor gene. Nat Med 4:1152-1156

84. Susulic VS, Frederich RC, Lawitts J, Tozzo E, Kahn BB, Harper ME, Himms-Hagen J, Flier JS, Lowell BB 1995 Targeted disruption of the beta 3-adrenergic receptor gene. J Biol Chem 270:29483-29492

85. Bachman ES, Dhillon H, Zhang CY, Cinti S, Bianco AC, Kobilka BK, Lowell BB 2002 betaAR signaling required for diet-induced thermogenesis and obesity resistance. Science 297:843-845

86. Gnacinska M, Malgorzewicz S, Guzek M, Lysiak-Szydlowska W, Sworczak K 2010 Adipose tissue activity in relation to overweight or obesity. Endokrynol Pol 61:160-168

87. Voss-Andreae A, Murphy JG, Ellacott KL, Stuart RC, Nillni EA, Cone RD, Fan W 2007 Role of the central melanocortin circuitry in adaptive thermogenesis of brown adipose tissue. Endocrinology 148:1550-1560

88. Farooqi IS, Drop S, Clements A, Keogh JM, Biernacka J, Lowenbein S, Challis BG, O'Rahilly S 2006 Heterozygosity for a POMC-null mutation and increased obesity risk in humans. Diabetes 55:2549-2553

89. Farooqi IS, O'Rahilly S 2008 Mutations in ligands and receptors of the leptin-melanocortin pathway that lead to obesity. Nat Clin Pract Endocrinol Metab 4:569-577

90. Cone RD 2005 Anatomy and regulation of the central melanocortin system. Nat Neurosci 8:571-578

91. Lloyd DJ, Bohan S, Gekakis N 2006 Obesity, hyperphagia and increased metabolic efficiency in Pc1 mutant mice. Hum Mol Genet 15:1884-1893

92. Creemers JW, Lee YS, Oliver RL, Bahceci M, Tuzcu A, Gokalp D, Keogh J, Herber S, White A, O'Rahilly S, Farooqi IS 2008 Mutations in the amino-terminal region of proopiomelanocortin (POMC) in patients with early-onset obesity impair POMC sorting to the regulated secretory pathway. J Clin Endocrinol Metab 93:4494-4499

93. Stutzmann F, Tan K, Vatin V, Dina C, Jouret B, Tichet J, Balkau B, Potoczna N, Horber F, O'Rahilly S, Farooqi IS, Froguel P, Meyre D 2008 Prevalence of melanocortin-4 receptor deficiency in Europeans and their age-dependent penetrance in multigenerational pedigrees. Diabetes 57:2511-2518

94. Fox DL, Good DJ 2008 Nhlh2 Interacts with STAT3 to Regulate Transcription of Prohormone Convertase 1/3. Mol Endocrinol

95. Sutton GM, Trevaskis JL, Hulver MW, McMillan RP, Markward NJ, Babin MJ, Meyer EA, Butler AA 2006 Diet-genotype interactions in the development of the obese, insulin-resistant phenotype of C57BL/6J mice lacking melanocortin-3 or -4 receptors. Endocrinology 147:2183-2196

96. Cogliati T, Delgado-Romero P, Norwitz ER, Guduric-Fuchs J, Kaiser UB, Wray S, Kirsch IR 2007 Pubertal impairment in Nhlh2 null mice is associated with hypothalamic and pituitary deficiencies. Mol Endocrinol 21:3013-3027

97. Brown L, Espinosa R, 3rd, Le Beau MM, Siciliano MJ, Baer R 1992 HEN1 and HEN2: a subgroup of basic helix-loop-helix genes that are coexpressed in a human neuroblastoma. Proc Natl Acad Sci U S A 89:8492-8496

98. O'Rahilly S, Gray H, Humphreys PJ, Krook A, Polonsky KS, White A, Gibson S, Taylor K, Carr C 1995 Brief report: impaired processing of prohormones associated with abnormalities of glucose homeostasis and adrenal function. N Engl J Med 333:1386-1390

99. Jackson RS, Creemers JW, Ohagi S, Raffin-Sanson ML, Sanders L, Montague CT, Hutton JC, O'Rahilly S 1997 Obesity and impaired prohormone processing associated with mutations in the human prohormone convertase 1 gene. Nat Genet 16:303-306

100. Yeo GS, Farooqi IS, Aminian S, Halsall DJ, Stanhope RG, O'Rahilly S 1998 A frameshift mutation in MC4R associated with dominantly inherited human obesity. Nat Genet 20:111-112

101. Vaisse C, Clement K, Durand E, Hercberg S, Guy-Grand B, Froguel P 2000 Melanocortin-4 receptor mutations are a frequent and heterogeneous cause of morbid obesity. J Clin Invest 106:253-262

102. Cox JE, Laughton WB, Powley TL 1985 Precise estimation of carcass fat from total body water in rats and mice. Physiol Behav 35:905-910

103. Zhu X, Orci L, Carroll R, Norrbom C, Ravazzola M, Steiner DF 2002 Severe block in processing of proinsulin to insulin accompanied by elevation of des-64,65 proinsulin intermediates in islets of mice lacking prohormone convertase 1/3. Proc Natl Acad Sci U S A 99:10299-10304

104. Davalli AM, Perego L, Bertuzzi F, Finzi G, La Rosa S, Blau A, Placidi C, Nano R, Gregorini L, Perego C, Capella C, Folli F 2008 Disproportionate hyperproinsulinemia, beta-cell restricted prohormone convertase 2 deficiency, and cell cycle inhibitors expression by human islets transplanted into athymic nude mice: insights into nonimmune-mediated mechanisms of delayed islet graft failure. Cell Transplant 17:1323-1336

105. Mazumder PK, O'Neill BT, Roberts MW, Buchanan J, Yun UJ, Cooksey RC, Boudina S, Abel ED 2004 Impaired cardiac efficiency and increased fatty acid oxidation in insulin-resistant ob/ob mouse hearts. Diabetes 53:2366-2374

106. Lin J, Tarr PT, Yang R, Rhee J, Puigserver P, Newgard CB, Spiegelman BM 2003 PGC-1beta in the regulation of hepatic glucose and energy metabolism. J Biol Chem 278:30843-30848

107. Lin J, Yang R, Tarr PT, Wu PH, Handschin C, Li S, Yang W, Pei L, Uldry M, Tontonoz P, Newgard CB, Spiegelman BM 2005 Hyperlipidemic effects of dietary saturated fats mediated through PGC-1beta coactivation of SREBP. Cell 120:261-273

108. Coll T, Rodriguez-Calvo R, Barroso E, Serrano L, Eyre E, Palomer X, Vazquez-Carrera M 2009 Peroxisome proliferator-activated receptor (PPAR) beta/delta: a new potential therapeutic target for the treatment of metabolic syndrome. Curr Mol Pharmacol 2:46-55

109. Challis BG, Coll AP, Yeo GS, Pinnock SB, Dickson SL, Thresher RR, Dixon J, Zahn D, Rochford JJ, White A, Oliver RL, Millington G, Aparicio SA, Colledge WH, Russ AP, Carlton MB, O'Rahilly S 2004 Mice lacking pro-opiomelanocortin are sensitive to high-fat feeding but respond normally to the acute anorectic effects of peptide-YY(3-36). Proc Natl Acad Sci U S A 101:4695-4700

110. Yaswen L, Diehl N, Brennan MB, Hochgeschwender U 1999 Obesity in the mouse model of pro-opiomelanocortin deficiency responds to peripheral melanocortin. Nat Med 5:1066-1070

111. Fox DL, Fox DLG, R.V. J, Good DJ 2007 Microarray Technology Uncovers Biological Pathways Involved in the Development of Obesity in

Nhlh2 Knockout Mice. In: Thangadurai D TW, and Pullaiah T ed. Genes, Genomes and Genomics. New Delhi: Regency Publications

112. Ahituv N, Kavaslar N, Schackwitz W, Ustaszewska A, Martin J, Hebert S, Doelle H, Ersoy B, Kryukov G, Schmidt S, Yosef N, Ruppin E, Sharan R, Vaisse C, Sunyaev S, Dent R, Cohen J, McPherson R, Pennacchio LA 2007 Medical sequencing at the extremes of human body mass. Am J Hum Genet 80:779-791

113. Goren A, Kim E, Amit M, Bochner R, Lev-Maor G, Ahituv N, Ast G 2007 Alternative approach to a heavy weight problem. Genome Res

114. Henkin L, Bergman RN, Bowden DW, Ellsworth DL, Haffner SM, Langefeld CD, Mitchell BD, Norris JM, Rewers M, Saad MF, Stamm E, Wagenknecht LE, Rich SS 2003 Genetic epidemiology of insulin resistance and visceral adiposity. The IRAS Family Study design and methods. Ann Epidemiol 13:211-217